

000 001 002 003 004 005 006 007 008 009 010 011 012 013 014 015 016 017 018 019 020 021 022 023 024 025 026 027 028 029 030 031 032 033 034 035 036 037 038 039 040 041 042 043 044 045 046 047 048 049 050 051 052 053 LEARN THE ROPES, THEN TRUST THE WINS: SELF-IMITATION WITH PROGRESSIVE EXPLORATION FOR AGENTIC REINFORCEMENT LEARNING

Anonymous authors

Paper under double-blind review

ABSTRACT

Reinforcement learning (RL) is the dominant paradigm for sharpening strategic tool use capabilities of LLMs on long-horizon, sparsely-rewarded agent tasks, yet it faces a fundamental challenge of exploration-exploitation trade-off. Existing studies stimulate exploration through the lens of policy entropy, but such mechanical entropy maximization is prone to RL instability due to the multi-turn distribution shifting. In this paper, we target the progressive exploration-exploitation balance under the guidance of the agent’s own experiences without succumbing to either entropy collapsing or runaway divergence. We propose SPEAR , a self-imitation learning (SIL) recipe for training agentic LLMs. It extends the vanilla SIL, where a replay buffer stores good experience for off-policy update, by gradually steering the policy entropy across stages. Specifically, the proposed curriculum scheduling harmonizes intrinsic reward shaping and self-imitation to 1) expedite exploration via frequent tool interactions at the beginning, and 2) strengthen exploitation of successful tactics upon convergence towards familiarity with the environment. We also combine bag-of-tricks of industrial RL optimizations for a strong baseline Dr.BoT to demonstrate our effectiveness. In ALFWorld and WebShop, SPEAR increases the success rates of GRPO/GiGPO/Dr.BoT by up to 16.1%/5.1%/8.6% and 20.7%/11.8%/13.9%, respectively. In AIME24 and AIME25, SPEAR boosts Dr.BoT by up to 3.8% and 6.1%, respectively. Such gains incur only 10%–25% extra theoretical complexity and negligible runtime overhead in practice, demonstrating the plug-and-play scalability of SPEAR.

1 INTRODUCTION

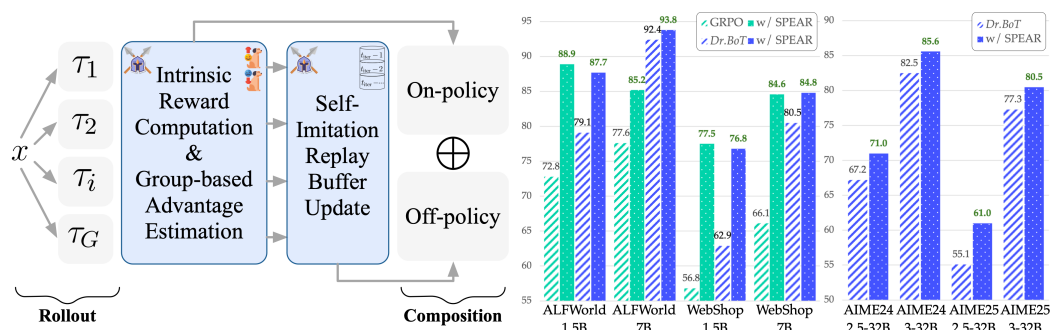


Figure 1: Our SPEAR harmonizes the curriculum-scheduled self-imitation learning with intrinsic reward shaping for progressive exploration, improving policy performance across agentic tasks.

Reinforcement Learning (RL) (Lambert et al., 2024; Guo et al., 2025; Qin et al., 2025b) has driven the development of reasoning capabilities of Large Language Models (LLMs). Built upon the reason-and-act (ReAct) paradigm (Yao et al., 2023), LLMs have powered various agentic applications such as simulated robot navigation (Shridhar et al., 2020; Li et al., 2024), mobile assistant (Wang et al., 2024; Li et al., 2025a), web navigator (Furuta et al., 2023; He et al., 2024), deep

searcher (Jin et al., 2025b; Li et al., 2025c; Tao et al., 2025), and GUI master (Qin et al., 2025a; Hong et al., 2024). A fundamental challenge in applying RL to LLM agents is to manage the balance between exploration and exploitation. The LLM agent needs to *exploit* both pretrained knowledge and past interactions to formalize experience that maximize rewards. At the same time, it must *explore* novel behaviors through tool-integrated reasoning and reflection. The interweaving between exploration and exploitation determines the emerging agent’s competence upon convergence.

Existing studies often quantify the exploration potential through entropy (Sutton, 1988; Williams & Peng, 1991; Cui et al., 2025b; Xue et al., 2025), where the decline of policy entropy indicates **overconfidence with insufficient exploration**. In this case, a series of regularization techniques (Ziebart et al., 2008; Schulman et al., 2017b; Haarnoja et al., 2018) have been proposed to maximize entropy (Haarnoja et al., 2017; Zhao et al., 2019; Xin et al., 2020; Zhang et al., 2021; Seo et al., 2021; Mehr et al., 2023; Kim & Sung, 2023; Hao et al., 2023). However, when it comes to LLM-driven agents, entropy-based control is fragile: the accumulation of low-probability tokens from the environment feedback induces severe distribution shifting, often leading to mode collapse (Xue et al., 2025; Dong et al., 2025b). **Agent** models may experience sustained entropy growth due to uncertainty about multi-turn interactions and training instability becomes frequent (Mai et al., 2025; Yao et al., 2025; Wang et al., 2025b). Recent approaches attempt to mitigate this issue by cold-start supervised fine-tuning (SFT) (Tao et al., 2025; Qin et al., 2025a; Feng et al., 2025a; Qin et al., 2025c) or hybrid schemes that combine RL with SFT (Zhang et al., 2025a). Although these methods improve stability, they compromise **policy’s discovery of** strategies beyond those present in the SFT corpus. This limitation highlights the need for adaptive training frameworks that can *dynamically schedule LLM-driven agents to decide when to explore and when to exploit*.

In this paper, we are trying to answer the following core research question: **Can we schedule a smooth transition between exploration and exploitation guided by the policy’s own experience without going to extremes of either entropy collapsing or runaway divergence?** We hypothesize that the agent should maintain its policy entropy within a dynamic but controlled range that evolves over time: 1) **At the early stages, increasing entropy is beneficial for broad skill-level exploration.** The agent is expected to rapidly develop tool-use capabilities, encounter unfamiliar observations, and engage in trial-and-errors. 2) **As training advances, however, a shift toward converging entropy is required.** This enables the agent to consolidate problem-solving heuristics and emphasize *action-level* exploration. The agent exploits reward signals to choose comparatively more effective actions and adapts to changing distributions for stabilizing its evolutionary path.

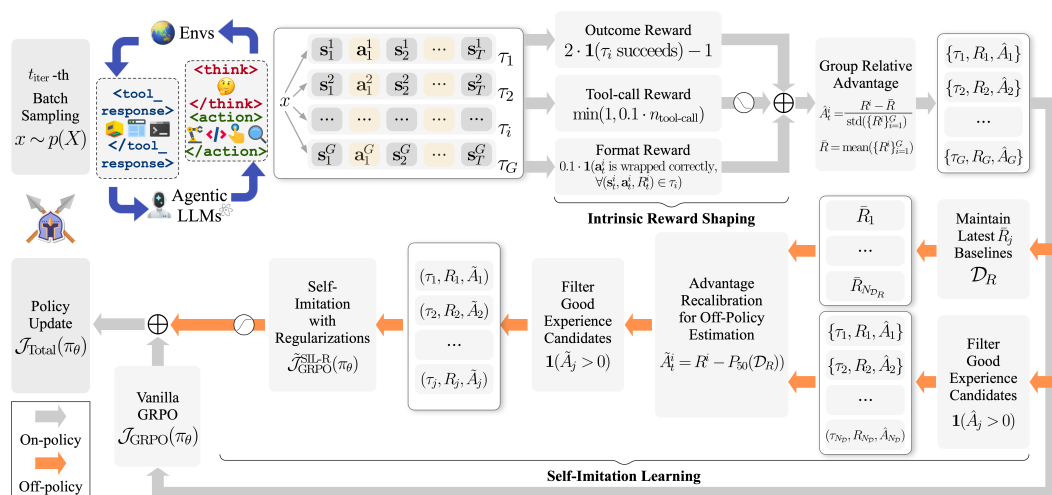


Figure 2: **Overview of SPEAR.** First, the agent interacts with the environment for a set of trajectories, which flow through intrinsic reward shaping and advantage estimation with on-policy updates. Second, they are selected and stored in a replay buffer, enabling off-policy updates via the proposed self-imitation scheme. This dual integration allows the maximal utility of past experiences, thereby expanding the effective exploration space, while simultaneously mitigating persistent uncertainty.

To address this, we propose the Self-imitation with Progressive Exploration for Agentic Reinforcement learning (**SPEAR**), a curriculum-based RL recipe for improving the *exploration-exploitation* balance with *self-imitation* and *intrinsic reward*. As shown in Figure 1, the core principle follows the vanilla Self-Imitation Learning (SIL) (Oh et al., 2018; Ferret et al., 2020) where an independent replay buffer is prepared to store the state-action pairs only when their returns in the past episodes exceed the baselines. Such a replay buffer is exploited to encourage actions with good returns and improve hard exploration based on these successful trajectories under the sparse-reward, long-horizon agent tasks. Specifically, we introduce three modifications to SIL tailored to the dynamics of policy entropy in agentic tasks. First, we incorporate a curriculum to integrate both *skill-level* and *action-level* exploration by adjusting reward shaping and self-imitation across stages. Second, we tackle the off-policy nature of the update with experiences in the buffer and avoid advantage recomputation by advantage recalibration. Third, we regularize policy updates to stabilize entropy and mitigate reward hacking. Finally, inspired by existing industrial bag-of-tricks, we present a strong baseline *Dr.BoT* for agentic RL training. Our SPEAR brings considerable performance gains to *GRPO/GiGPO* (Feng et al., 2025b)/*Dr.BoT* respectively up to *16.1%/5.1%/8.6%* on ALFWORLD (Shridhar et al., 2020) and *20.7%/11.8%/13.9%* on WebShop (Yao et al., 2022). It boosts our *Dr.BoT* respectively up to *3.8%* on AIME24 and *6.1%* on AIME25 (AIME, 2025). These gains come with around $10\% \sim 25\%$ computation overhead in theoretical complexity, but end up with quite comparable runtime per iteration in practice. Such compatibility and scalability enable SPEAR a plug-and-play algorithm for training versatile agents. In summary, our contributions are:

- 1) We propose SPEAR, a generalization of the SIL for training LLM agents. It bypasses the costly expert imitation and allows exploration under the guidance of one’s own rewarded experience.
- 2) We bring in curriculum scheduling to harmonize SIL with intrinsic reward shaping for policy entropy management and progressive transition from *skill-based* to *action-based* exploration.
- 3) We propose a strong baseline, *Dr.BoT*, which combines established RL techniques validated in industrial practice, confirming its effectiveness and superiority over existing baselines.

2 RELATED WORK

2.1 REINFORCEMENT LEARNING ALGORITHMS FOR LLMs

With the advent of large-scale reasoning models (Jaech et al., 2024), Reinforcement Learning (RL) (Ouyang et al., 2022) has been adopted more broadly. Proximal Policy Optimization (PPO) (Schulman et al., 2017b) leverages an actor-critic architecture together with the clipped surrogate objective and a Kullback–Leibler (KL) divergence penalty to constrain policy update. Group Relative Policy Optimization (GRPO) (Guo et al., 2025; Shao et al., 2024) simplifies this setup by replacing the critic with a group-wise baseline. Building on GRPO, DAPO (Yu et al., 2025) uses dynamic sampling and “clip higher” to encourage exploration and stabilize training. Dr.GRPO (Liu et al., 2025b) addresses length bias and the difficulty bias. Existing methods have greatly advanced RL for LLMs. However, naively combining them can lead to conflicts or tight couplings among techniques. To this end, we harmonize the strengths of DAPO, Dr.GRPO, and other agent studies from research and industrial practice to establish a strong baseline, *Dr.BoT*, as detailed in Section 4.4.

2.2 OPTIMIZATION OF LLM AGENTS

Recent researches investigate how to endow models with better tool-use capabilities (Feng et al., 2025a; Li et al., 2025d; Xue et al., 2025). LLMs are optimized to strengthen information seeking from open web (Jin et al., 2025b; Tao et al., 2025; Gao et al., 2025). RAGEN (Wang et al., 2025b) improves the stability of multi-turn RL through instance filtering and gradient shaping. GiGPO (Feng et al., 2025b) augments group-level advantages with additional step-level advantage estimates. ARPO (Dong et al., 2025b) monitors entropy dynamics during rollouts to branch trajectories adaptively. In this work, we address the exploration-exploitation dilemma under multi-turn tool-use settings. We introduce a curriculum-regulated RL regime that gradually shifts skill-based exploration towards action-based exploration. We integrate self-imitation and intrinsic reward to consolidate successful behaviors (Section 4.2). Our SPEAR can work with existing algorithms in a plug-and-play manner, exhibiting a high level of compatibility and generalization.

162 2.3 EXPLORATION IN REINFORCEMENT LEARNING
163

164 Curiosity-driven methods (Pathak et al., 2017; Houthooft et al., 2016) grant intrinsic rewards for pre-
165 diction error or novelty to actively seek unfamiliar states. Count-based algorithms (Bellemare et al.,
166 2016; Tang et al., 2017) introduce pseudo-counts derived from a density model to assign count-based
167 bonuses. Skill acquisition methods (Gregor et al., 2016; Eysenbach et al., 2018) discover distinct
168 options by maximizing the mutual information. Entropy-regularization methods (Haarnoja et al.,
169 2018; Cui et al., 2025b) maximize the expected reward and entropy of the policy. However, tradi-
170 tional exploration techniques can lead to divergence of agent LLMs as the multi-turn interactions
171 already result in the increased uncertainty on unfamiliar observations. Under such circumstance,
172 we propose the curriculum-guided self-imitation to leverage the agent’s own experience for balanc-
173 ing exploration and exploitation. It avoids handcrafted heuristic techniques in previous studies and
174 instead fully relies on the agent itself to reinforce successful and valid patterns.

175 2.4 EXPERIENCE REPLAY IN REINFORCEMENT LEARNING
176

177 Self-Imitation Learning (SIL) (Oh et al., 2018) takes advantage of past successful experience to
178 drive its future learning (Schaul et al., 2015; Horgan et al., 2018; Gangwani et al., 2018; Pan et al.,
179 2022; Saglam et al., 2023). SAIL (Ferret et al., 2020) extends SIL to off-policy, action value-
180 based RL methods. Tang (2020) proves that SIL’s return-based update provides a bias–variance
181 trade-off that speeds up learning. SILfD (Pshikhachev et al., 2022) extends SIL to leverage both
182 external demonstrations and the agent’s own experience. GSIL (Xiao et al., 2024) proposes an
183 offline alignment framework that uses self-imitation on demonstration data. While SIL benefits
184 long-horizon problems, its induces entropy collapsing to agent RL. To mitigate this, we harmonize
185 both self-imitation and intrinsic reward with curriculum scheduling for progressive exploration.

186 3 PRELIMINARIES
187188 3.1 PROBLEM DEFINITION
189

190 Given a task $x \sim p(X)$ where $p(X)$ represents data distribution, an LLM agent parameterized by
191 θ interacts with the environment E until it completes the task or exceeds the max number of turns
192 T . It can be modeled by Markov Decision Process (MDP) where s_t , a_t , and R_t respectively denote
193 the state, action, and reward at time t . Given a full episode $\tau = \{(s_1, a_1, R_1), (s_2, a_2, R_2), \dots\}$, we
194 aim to optimize the agent policy π_θ . Following previous studies (Dong et al., 2025a; Feng et al.,
195 2025b;a; Dong et al., 2025b), we define three distinct types of actions (see Appendix A.2).

196 3.2 POLICY OPTIMIZATION
197

198 We adopt the GRPO (Shao et al., 2024) which stems from PPO (Schulman et al., 2017a;b) but
199 replaces the model-based A (Schulman et al., 2015) with the group-based \hat{A} (Appendix A.3).

200 4 TRAINING AGENTIC LLMs WITH SPEAR 
201202 4.1 PRELIMINARY FINDINGS
203

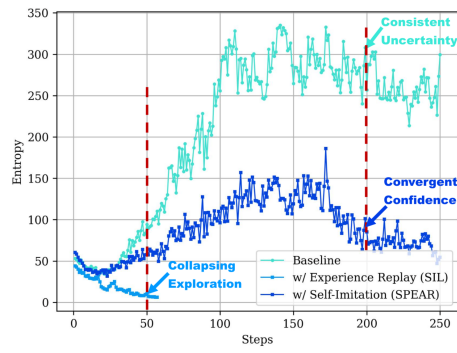
204 The extension of SIL to LLM-driven agents faces entropy collapse. Figure 3 illustrates that the over-
205 fitting of the few available successful experience causes irreversible stagnation of exploration. In ad-
206 dition, we demonstrate that the inclusion of the tool-call reward is a double-edged sword (Figure 4),
207 where the competition between reward terms causes the oscillations to converge. To address these
208 challenges, we introduce SPEAR for progressive exploration with self-imitation (Algorithm 1).

209 4.2 SELF-IMITATION LEARNING
210

211 We resort to self-imitation to unearth past successful experience for effective *action-level* explo-
212 ration, where the agent learns novel strategies along the promising decision path instead of random
213 walk and bifurcation. We prevent policy entropy divergence by replaying rewarded trajectories.

216

217



228 (a) Entropy (seq-mean-token-sum-norm).

229

230

231 Figure 3: Effect of our self-imitation on action-level strategy exploration (Qwen2.5-32B with code
 232 interpreter). The vanilla experience replay technique (Oh et al., 2018) that enforces early overfitting
 233 of the few available trajectories in the buffer causes entropy collapsing and exploration shrinkage.
 234 At the beginning, the LLM agent struggles at tool-calling skills and fails to cultivate the transition
 235 of distribution towards frequent tool utilization and tool-integrated reasoning. The naive replay lim-
 236 its the transformation of reasoning paradigm. In contrast, our SPEAR introduces both curriculum-
 237 and covariance- based regularization into self-imitation. Its curriculum schedule with an increasing
 238 emphasis on the replay data allows easy acquisition of tool-use skills at first, and stimulates strategic
 239 action plans later. The covariance clipping removes over-confident tokens, whose log probabili-
 240 ties are highly associated with their advantage gains, out of optimization. Our self-imitation gives
 241 promises to exploring novel strategies and achieves steady growth on AIME 2025.

242

243

244

245

Prioritized Experience Replay in Self-Imitation. A replay buffer is maintained to store previous trajectories, their rewards and advantages $\mathcal{D} = \{(\tau_j, R_j, \hat{A}_j)\}, j = 1, 2, \dots, N_{\mathcal{D}}$ where $N_{\mathcal{D}}$ denotes the buffer size. To exploit only good trajectories, we keep those with positive advantages:

246

247

248

$$\mathcal{J}_{\text{GRPO}}^{\text{SIL}}(\pi_{\theta}) = \mathbb{E}_{\{\tau_j\}_{j=1}^{N_{\mathcal{D}}} \sim \{\pi_{\theta_{\text{old}}}(\cdot|x), x \sim p(X)\}} \sum_{j=1}^{N_{\mathcal{D}}} \mathcal{J}_{\text{GRPO}}^j \cdot \mathbf{1}(\hat{A}_j > 0), \quad (1)$$

249

250

251

where the indicator $\mathbf{1}(\cdot)$ equals to 1 when the condition satisfied and 0 otherwise. The past trajectories not only come from the last policy $\pi_{\theta_{\text{old}}}$ but also the policies $\{\pi_{\theta_{\text{old}}}\}$ of few steps earlier.

252

253

254

255

256

257

258

259

260

261

262

263

264

265

266

Advantage Recalibration for Off-Policy Estimation. We propose to recalibrate the advantage of trajectories in the buffer to address the underlying off-policy challenge. That is to say, the observed return of a trajectory from the past policy becomes increasingly different from the current one, under the assumption that the policy keeps improving during iterations (Ferret et al., 2020; Luo et al., 2021). Under this assumption, vanilla SIL computes the advantage with a pointwise max with the per-state empirical return as a baseline, which can be seen as a proxy for the upper-envelope projection of the value function onto empirical returns. GRPO removes the learned value baseline by estimating the state-dependent baseline performance through its reliance on intra-group reward averaging, but this still depends on the target policy and requires extra computation resources for sampling. **Dynamic adjustment on the baseline performance is performed to calibrate relative gains without introducing additional computing.** Specifically, we maintain a First-In-First-Out (FIFO) buffer of intra-group baselines for the latest $N_{\mathcal{D}_R}$ trajectories $\mathcal{D}_R = \{\bar{R}_j\}_{j=1}^{N_{\mathcal{D}_R}}$ where $N_{\mathcal{D}_R}$ denotes the size of the baseline buffer. As training progresses, due to the high variance nature of agentic RL, we utilize the 50-th percentile $P_{50}(\mathcal{D}_R)$ as a conservative but robust estimation of the policy baseline with either upward or downward trends. To bypass the inaccurate estimation of intra-group standard deviation, we follow (Liu et al., 2025b) to simply remove such a term in advantage computation:

267

268

269

$$\tilde{A}_t^i = R^i - P_{50}(\mathcal{D}_R). \quad (2)$$

Such recalibrated advantage enjoys three benefits: 1) the baseline performance correlates with the policy change; 2) the outdated experiences can be filtered out with both $\hat{A}_j > 0$ and $\tilde{A}_j > 0$; 3) the

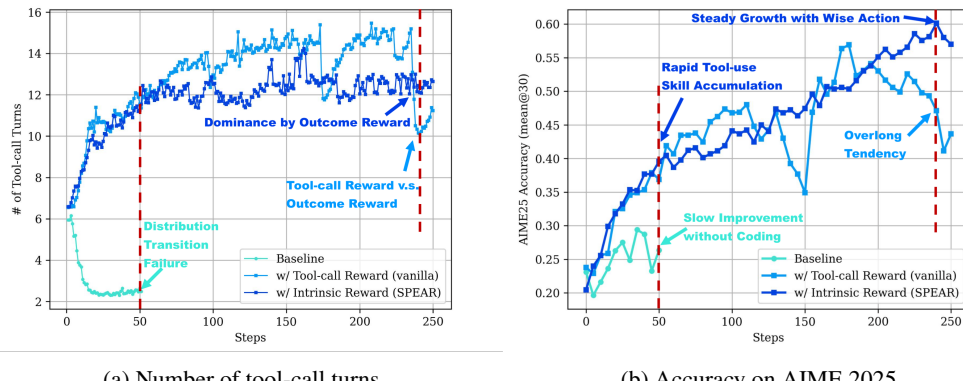
270 difficulty bias by group normalization can be mitigated. The updated off-policy SIL objective is:
 271

$$272 \tilde{\mathcal{J}}_{\text{GRPO}}^{\text{SIL}}(\pi_\theta) = \mathbb{E}_{\{\tau_j\}_{j=1}^{N_{\mathcal{D}}} \sim \{\pi_{\theta_{\text{old}}}(\cdot|x), x \sim p(X)\}} \sum_{j=1}^{N_{\mathcal{D}}} \tilde{\mathcal{J}}_{\text{GRPO}}^j \cdot \mathbf{1}(\hat{A}_j > 0 \& \tilde{A}_j > 0), \quad (3)$$

$$273 \tilde{\mathcal{J}}_{\text{GRPO}}^i = \left[\frac{1}{T} \sum_{t=1}^T (\min(r_t^i(\theta) \tilde{A}_t^i, \text{clip}(r_t^i(\theta), 1-\epsilon, 1+\epsilon) \tilde{A}_t^i) - \beta D_{\text{KL}}^i(\pi_\theta || \pi_{\text{ref}}) \right]. \quad (4)$$

274
 275 **Progressive Experience Utilization with Curriculum Schedule.** We perform scheduling to 1)
 276 restrict mechanical imitation of probable-yet-immature experience at an early stage, and 2) prevent
 277 consistent uncertainty about the environment states and policy actions at later stage. We apply a
 278 warm-up γ on the SIL term under the assumption that initially the transition of distribution towards
 279 diverse actions outweighs the imitation of limited solution patterns (see Equation 13 and Figure 6a).
 280

$$281 \mathcal{J}_{\text{Total}}(\pi_\theta) = \mathcal{J}_{\text{GRPO}}(\pi_\theta) + \gamma \cdot \tilde{\mathcal{J}}_{\text{GRPO}}^{\text{SIL}}(\pi_\theta). \quad (5)$$



(a) Number of tool-call turns.

(b) Accuracy on AIME 2025.

301
 302 Figure 4: Effect of our intrinsic reward on skill-level strategy exploration (Qwen2.5-32B with code
 303 interpreter). The baseline does not consider tool-calling as a rewarded behavior and its number of
 304 interaction with the environment drops quickly due to the negative feedback of bad codes. In this
 305 case, the LLM gives up coding and degrades to text-based reasoning. The vanilla tool-call reward,
 306 despite being effective in learning tool-call skills at first, causes competition with the outcome re-
 307ward later. Due to the limited context length, the excessive tool-call turns prevents submission of the
 308 final answer and thereafter the accuracy declines immediately. We propose the curriculum schedule
 309 as an intrinsic reward design where its strength decays over step to allow the agent to merely focus
 310 on the accuracy with wiser actions. It prevents reward hacking for unnecessarily long interactions.
 311

312 4.3 INTRINSIC REWARD SHAPING

313 We resort to intrinsic reward for *skill-level* exploration where the agent is guided by a tool-call reward
 314 to broadly investigate tool usage. Such design not only benefits tool learning but more importantly
 315 stimulates interactions that familiarize the agent with the environment for experience accumulation.
 316

317 **Reward Composition.** A compound reward R^i of each trajectory τ_i not only considers the final
 318 outcome but also the behaviors that are promising to achieve the goal: an outcome accuracy reward
 319 R_{outcome}^i , a continuous tool-call reward $R_{\text{tool-call}}^i$, and a format reward R_{format}^i (see Appendix A.7).
 320

321 **Progressive Reward Modulation with Curriculum Schedule.** We regulate the contribution of
 322 tool call reward to: 1) accelerate the mastering of tool usage for quick distribution shifting towards
 323 new task settings at an early stage, and 2) prevent optimization oscillation and competition at a later

324 **stage.** Although previous studies (Qian et al., 2025; Li et al., 2023; Da et al., 2025; Xia et al., 2025;
 325 Singh et al., 2025; Wei et al., 2025; Gou et al., 2023; Lin & Xu, 2025) experimented with various
 326 auxiliary rewards, we show that the addition of tool-call reward is a double-edged sword. The
 327 agent trained without the tool-call reward fails to develop tool-integrated reasoning (Figure 4) due
 328 to negative tool response: 1) missing import of modules; 2) reference to undefined variables;
 329 3) unexpected indentation error; and 4) forgetting to print results. The agent quickly gives
 330 up coding to run away from errors and turns to pure textual reasoning. On the other hand, the
 331 enforcement of tool-call reward stimulates an increasing number of interaction turns, leading to over-
 332 long responses that cause oscillation to outcome accuracy. We alleviate the competition between
 333 reward terms by scheduling the tool-call reward with μ (Equation 14 and Figure 6b):

$$R^i = R_{\text{outcome}}^i + \mu \cdot R_{\text{tool-call}}^i + R_{\text{format}}^i. \quad (6)$$

336 4.4 *Dr.BoT* AS A STRONG BASELINE

338 To provide a strong baseline, we refer to the existing studies (Liu et al., 2025c; Sun et al., 2025; Bai
 339 et al., 2025a; Cui et al., 2025b) for diverse exploration, stable convergence, and effective training.
 340 Our baseline, *Dr.BoT*, consists of bag-of-tricks modifications to the GRPO (see Appendix A.8).

341 Table 1: Results on ALFWorld & WebShop (%). PT & FW stand for prompting & framework.
 342

343 Type	Method	344 ALFWorld						345 WebShop		
		346 Pick	347 Look	348 Clean	349 Heat	350 Cool	351 Pick2	352 All	353 Score	354 SR
<i>Qwen2.5-1.5B-Instruct</i>										
355 PT	I/O	5.9	5.5	3.3	9.7	4.2	0.0	4.1	23.1	5.2
356 FW	ReAct	17.4	20.5	15.7	6.2	7.7	2.0	12.8	40.1	11.3
357 FW	Reflexion	35.3	22.2	21.7	13.6	19.4	3.7	21.8	55.8	21.9
358 RL	PPO	64.8	40.5	57.1	60.6	46.4	47.4	54.4	73.8	51.5
359 RL	RLOO	88.3	52.8	71.0	62.8	66.4	56.9	69.7	73.9	52.1
360 RL	GRPO	85.3	53.7	84.5	78.2	59.7	53.5	72.8	75.8	56.8
361 RL	+ SPEAR (ours)	93.9	80.9	96.4	87.4	88.3	79.1	88.9 _(+16.1%)	90.0	77.5 _(+20.7%)
362 RL	<i>Dr.BoT</i> (GRPO)	92.2	75.8	81.0	81.8	72.8	61.9	79.1	78.7	62.9
363 RL	+ SPEAR (ours)	91.2	72.2	94.1	95.1	88.3	74.4	87.7 _(+8.6%)	88.4	76.8 _(+13.9%)
364 RL	GiGPO w/std	94.4	67.5	94.8	94.4	79.8	76.4	86.7	83.1	65.0
365 RL	GiGPO w/o std	96.0	76.5	91.8	91.3	71.7	79.5	86.1	83.5	67.4
366 RL	+ SPEAR (ours)	95.2	79.2	89.1	94.0	88.8	95.5	91.2 _(+5.1%)	90.7	79.3 _(+11.8%)
367 RL	<i>Dr.BoT</i> (GiGPO)	98.6	91.4	93.7	93.8	85.4	78.4	90.6	84.1	68.8
368 RL	+ SPEAR (ours)	96.4	86.5	96.1	99.0	87.6	91.6	93.2 _(+2.6%)	90.9	81.1 _(+12.2%)
<i>Qwen2.5-7B-Instruct</i>										
369 PT	I/O	33.4	21.6	19.3	6.9	2.8	3.2	14.8	26.4	7.8
370 FW	ReAct	48.5	35.4	34.3	13.2	18.2	17.6	31.2	46.2	19.5
371 FW	Reflexion	62.0	41.6	44.9	30.9	36.3	23.8	42.7	58.1	28.8
372 RL	PPO	92.3	64.0	92.5	89.5	80.3	68.8	80.4	81.4	68.7
373 RL	RLOO	87.6	78.2	87.3	81.3	71.9	48.9	75.5	80.3	65.7
374 RL	GRPO	90.8	66.1	89.3	74.7	72.5	64.7	77.6	79.3	66.1
375 RL	+ SPEAR (ours)	93.7	62.4	97.2	78.0	83.1	75.5	85.2 _(+7.6%)	92.4	84.6 _(+18.5%)
376 RL	<i>Dr.BoT</i> (GRPO)	99.9	95.8	93.8	92.8	90.4	80.6	92.4	90.4	80.5
377 RL	+ SPEAR (ours)	98.8	97.9	97.1	88.5	89.2	87.2	93.8 _(+1.4%)	91.4	84.8 _(+4.3%)
378 RL	GiGPO w/std	97.7	82.7	98.8	83.7	89.3	79.2	90.8	84.4	72.8
379 RL	GiGPO w/o std	91.8	88.6	95.9	90.2	86.5	85.2	90.2	86.2	75.2
380 RL	+ SPEAR (ours)	99.9	82.4	98.0	92.8	92.6	86.6	94.1 _(+3.9%)	92.7	83.8 _(+8.6%)
381 RL	<i>Dr.BoT</i> (GiGPO)	98.3	99.9	96.9	92.8	91.8	88.3	94.0	90.7	81.8
382 RL	+ SPEAR (ours)	99.9	85.1	95.6	96.4	89.9	95.1	94.7 _(+0.7%)	92.5	85.7 _(+3.9%)

383 5 EXPERIMENTS

384 5.1 EXPERIMENTAL SETUP

385 Three benchmarks are used: ALFWorld (Shridhar et al., 2020), WebShop (Yao et al., 2022), and
 386 DAPO-MATH-17K (Yu et al., 2025) (Appendix A.10). According to these benchmarks, we respec-
 387 tively follow (Feng et al., 2025b) and (Feng et al., 2025a) to report a range of competitive baselines
 388 (Appendix A.11). All the training settings and hyper-parameters are detailed in Appendix A.12.

389 5.2 PERFORMANCE

390 Table 1 demonstrates our effectiveness on ALFWorld and WebShop. It is compatible with
 391 GRPO (Shao et al., 2024), GiGPO (Feng et al., 2025b), and our *Dr.BoT*. SPEAR brings consis-
 392 tent gains across 1.5B and 7B models up to 20%. Such generalization benefits from the collection of

378 successful trajectories, which acts as a walkthrough guide to the agent. Especially for tasks where
 379 the success rate is fairly low at the beginning, the agent has to figure out the underlying interaction
 380 logics and summarize action plans tailored specific to each task. The experience replay expedites
 381 the accumulation of tactics and thereafter reduces blind trials and errors. Furthermore, our *Dr:BoT*
 382 boosts GRPO and GiGPO up to 15%, showcasing the validity of mixture of tricks.
 383

384 Table 2: Results (mean@30) on AIME 2024 & 2025 (%). \dagger : Official implementation already utilizes
 385 DAPO tricks. \ddagger : Official results reported by Qwen (Yang et al., 2025). PT stands for prompting.

Type	Method	Model	Tool	Context Train	Context Test	AIME24	AIME25
PT	I/O	<i>Qwen2.5-32B-Instruct</i>	—	—	16K	13.4	12.9
PT	I/O	<i>Qwen2.5-32B-Instruct</i>	CI	—	16K	29.6	23.1
RL	PPO \dagger	<i>Qwen2.5-32B-Instruct</i>	CI	16K	16K	—	55.0
RL	GRPO \dagger	<i>Qwen2.5-32B-Instruct</i>	CI	16K	16K	—	60.0
RL	ReTool	<i>Qwen2.5-32B-Instruct</i>	CI	16K	16K	67.0	49.3
RL	SimpleTIR	<i>Qwen2.5-32B-Instruct</i>	CI	12K	12K	59.9	49.2
RL	ZeroTIR	<i>Qwen2.5-32B-Instruct</i>	CI	8K	8K	56.7	33.3
RL	AFM	<i>Qwen2.5-32B-Instruct</i>	CI	32K	32K	66.7	59.8
RL	<i>Dr:BoT</i> (GRPO)	<i>Qwen2.5-32B-Instruct</i>	CI	16K	16K	64.7	54.0
RL	+ SPEAR (ours)	<i>Qwen2.5-32B-Instruct</i>	CI	16K	16K	66.3 $(+1.6\%)$	60.1 $(+6.1\%)$
RL	<i>Dr:BoT</i> (GRPO)	<i>Qwen2.5-32B-Instruct</i>	CI	32K	32K	67.2	55.1
RL	+ SPEAR (ours)	<i>Qwen2.5-32B-Instruct</i>	CI	32K	32K	71.0 $(+3.8\%)$	61.0 $(+5.9\%)$
PT	I/O	<i>Qwen3-32B-Instruct</i>	—	—	16K	68.5	53.5
PT	I/O \ddagger	<i>Qwen3-32B-Instruct</i>	—	—	38K	81.4	72.9
PT	I/O	<i>Qwen3-32B-Instruct</i>	CI	—	16K	31.1	24.4
RL	<i>Dr:BoT</i> (GRPO)	<i>Qwen3-32B-Instruct</i>	CI	16K	16K	81.3	74.1
RL	+ SPEAR (ours)	<i>Qwen3-32B-Instruct</i>	CI	16K	16K	81.8 $(+0.5\%)$	78.8 $(+4.7\%)$
RL	<i>Dr:BoT</i> (GRPO)	<i>Qwen3-32B-Instruct</i>	CI	32K	32K	82.5	77.3
RL	+ SPEAR (ours)	<i>Qwen3-32B-Instruct</i>	CI	32K	32K	85.6 $(+3.1\%)$	80.5 $(+3.2\%)$

402 Table 2 reports the performance of CI-integrated reasoning on AIME24 and AIME25. *Dr:BoT* indeed
 403 outperforms recent RL baselines. The reduced context length of Qwen3 impedes complete reasoning
 404 and answer parsing. The agent learns to exploit the CI feedback for double-check and self-reflection.
 405 SPEAR achieves comparable performance with Qwen3 but using a much smaller token budget.
 406 When the context is relaxed to 32K, an improvement is observed on both Qwen2.5 and Qwen3,
 407 confirming our generalization with more interactions turns and reasoning tokens.

409 5.3 ABLATION STUDY

410 Table 3: Ablation on ALFWorld & WebShop. SI & IR stand for Self-Imitation & Intrinsic Reward.

Type	Method	ALFWorld						WebShop	
		Pick	Look	Clean	Heat	Cool	Pick2	All	Score
<i>Qwen2.5-1.5B-Instruct</i>									
RL	GRPO	85.3	53.7	84.5	78.2	59.7	53.5	72.8	75.8
RL	+ SI	86.8	61.0	87.4	87.7	71.1	56.6	77.3 $(+4.5\%)$	85.1
RL	+ SI + IR (SPEAR)	93.9	80.9	96.4	87.4	88.3	79.1	88.9 $(+16.1\%)$	90.0
RL	GiGPO w/o std	96.0	76.5	91.8	91.3	71.7	79.5	86.1	83.5
RL	+ SI	93.2	82.5	96.3	87.4	92.7	87.5	90.6 $(+4.5\%)$	89.4
RL	+ SI + IR (SPEAR)	95.2	79.2	89.1	94.0	88.8	95.5	91.2 $(+5.1\%)$	90.7
<i>Qwen2.5-7B-Instruct</i>									
RL	GRPO	90.8	66.1	89.3	74.7	72.5	64.7	77.6	79.3
RL	+ SI	93.2	82.5	96.3	87.4	92.7	87.5	90.6 $(+13.0\%)$	90.4
RL	+ SI + IR (SPEAR)	93.7	62.4	97.2	78.0	83.1	75.5	85.2 $(+7.6\%)$	92.4
RL	GiGPO w/o std	91.8	88.6	95.9	90.2	86.5	85.2	90.2	86.2
RL	+ SI	96.1	81.9	98.4	95.3	94.5	83.9	93.6 $(+3.4\%)$	94.6
RL	+ SI + IR (SPEAR)	99.9	82.4	98.0	92.8	92.6	86.6	94.1 $(+3.9\%)$	92.7

425 **Self-Imitation.** The SIL improves baselines consistently across model scales (Table 3). Since ei-
 426 ther 1.5B or 7B models perform poorly at the early stage (i.e., success rate $< 15\%$), past experiences
 427 are quite beneficial to explore promising strategies. The re-use of trajectories facilitates convergence
 428 and prevents mechanical trials especially for small agents. Table 4 shows that AIME24 dropped a
 429 bit by self-imitation but AIME25 still gets improved. Such fluctuation is related to the phenomenon
 430 (Figure 4) where the imitation of samples with multiple tool calls leads to rapid increase of interac-
 431 tion turns and thereafter causes training instability. The competition between different reward terms
 affects the robust selection of good experience, ultimately degrading the effectiveness of SIL.

Table 4: Ablation on AIME 2024 & 2025 (%). SI & IR stand for Self-Imitation & Intrinsic Reward.

Type	Method	Model	Tool	Context	AIME24	AIME25
				Train	Test	
RL	<i>Dr:BoT</i> (GRPO)	<i>Qwen2.5-32B-Instruct</i>	CI	16K	16K	64.7
RL	+ SI	<i>Qwen2.5-32B-Instruct</i>	CI	16K	16K	63.8(-0.9%)
RL	+ SI + IR (SPEAR)	<i>Qwen2.5-32B-Instruct</i>	CI	16K	16K	66.3(+1.6%)
RL	<i>Dr:BoT</i> (GRPO)	<i>Qwen2.5-32B-Instruct</i>	CI	32K	32K	67.2
RL	+ SI	<i>Qwen2.5-32B-Instruct</i>	CI	32K	32K	66.0(-1.2%)
RL	+ SI + IR (SPEAR)	<i>Qwen2.5-32B-Instruct</i>	CI	32K	32K	71.0(+3.8%)
RL	<i>Dr:BoT</i> (GRPO)	<i>Qwen3-32B-Instruct</i>	CI	16K	16K	81.3
RL	+ SI	<i>Qwen3-32B-Instruct</i>	CI	16K	16K	81.2(-0.1%)
RL	+ SI + IR (SPEAR)	<i>Qwen3-32B-Instruct</i>	CI	16K	16K	81.8(+0.5%)
RL	<i>Dr:BoT</i> (GRPO)	<i>Qwen3-32B-Instruct</i>	CI	32K	32K	82.5
RL	+ SI	<i>Qwen3-32B-Instruct</i>	CI	32K	32K	81.8(-0.7%)
RL	+ SI + IR (SPEAR)	<i>Qwen3-32B-Instruct</i>	CI	32K	32K	85.6(+3.1%)
						80.5(+3.2%)

Intrinsic Reward. The rewarding of interaction turns benefit 1.5B models consistently (Table 3). Two 7B outliers are found where the self-imitation alone brings the most performance gains. Such exception might be related to both the task definition and the RL algorithm. One should experiment with different combinations in practice. Table 4 shows that the intrinsic reward is indispensable for both Qwen2.5 and 3 because it encourages transformation from text-based reasoning to tool-integrated reasoning. It promotes frequent tool calling and such rich observation signals motivate the agent to correct coding errors, check the validity of the answer, and reflect on alternative solutions.

5.4 GENERALIZATION ON VISION-LANGUAGE AGENTS

Table 5: Success rate (%) of the visual agent for playing Sokoban.

Type	Method	Sokoban
	<i>Qwen2.5-VL-3B-Instruct</i>	
PT	I/O	11.7
RL	GRPO	67.1
RL	+ SPEAR (ours)	86.7(+19.6%)
RL	<i>Dr:BoT</i> (GRPO)	76.0
RL	+ SPEAR (ours)	85.4(+9.4%)
RL	GiGPO w/ std	76.9
RL	GiGPO w/o std	81.0
RL	+ SPEAR (ours)	87.7(+6.7%)
RL	<i>Dr:BoT</i> (GiGPO)	81.3
RL	+ SPEAR (ours)	87.9(+6.6%)

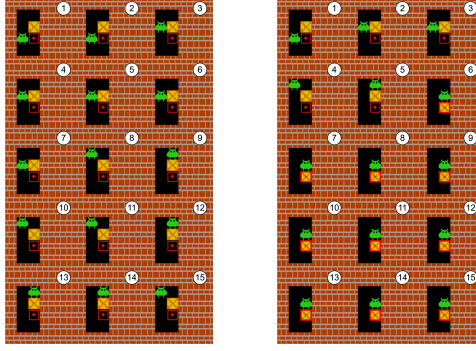


Figure 5: The agent learns to push the box.

To test whether the proposed SPEAR is still complimentary to existing GRPO-like algorithms on training visual agents, we follow (Feng et al., 2025b) to conduct experiments on the popular visual game Sokoban (Schrader, 2018). In this setting, the Qwen2.5-VL-3B-Instruct (Bai et al., 2025b) is adopted as the agentic LLM to solve the puzzle game where the player must push the boxes along the grid towards target positions without hitting the walls. It challenges the agent on spatial comprehension and long-term planning capabilities. The grid size is of 6×6 and the visual agent receives both the visual (RGB arrays) and textual inputs as states. As shown in Table 5, the proposed method generally improves the performance on Sokoban with either GRPO, GiGPO, and the proposed *Dr:BoT* baselines. At first, the visual agent is unaware of the winning logic behind the game and wanders around for "aimlessly" exploration (see Figure 5). After optimization, it not only comprehends the spatial relationship to control the box but also learns to stop moving when the task is completed.

5.5 GENERALIZATION ON SEARCH-AUGMENTED QA TASKS

To evaluate the performance of SPEAR on knowledge-intensive reasoning tasks, we conduct experiments on search-augmented QA tasks, including the single-hop QA datasets (NQ (Kwiatkowski et al., 2019), TriviaQA (Joshi et al., 2017), and PopQA (Mallen et al., 2023)) and multi-hop QA datasets (HotpotQA (Yang et al., 2018), 2Wiki (Ho et al., 2020), MuSiQue (Trivedi et al., 2022), and Bamboogle (Press et al., 2023)). We follow the experimental settings of SearchR1 (Jin et al.,

486
487
488 Table 6: Results on search-augmented QA Tasks.
489
490
491
492
493

Type	Method	Single-Hop QA				Multi-Hop QA			Avg.	
		NQ	TriviaQA	PopQA	HotpotQA	2Wiki	MuSiQue	Bamboogle		
<i>Qwen2.5-7B-Instruct</i>										
RL	Search-R1	39.3	61.0		39.7	37.0	40.1	14.6	36.8	38.5
RL	SPEAR	35.7	62.7		34.5	46.9	43.4	17.2	44.8	40.7
<i>Qwen2.5-14B-Instruct</i>										
RL	Search-R1	48.8	67.7		48.2	45.5	47.0	21.1	51.6	49.1
RL	SPEAR	47.6	69.3		47.8	48.5	48.8	26.7	56.6	49.3

2025b; Gao et al., 2025) to launch the local wiki-18 retrieval service. We adopt the Hierarchical Navigable Small World (HNSW) CPU indexing as approximation of nearest neighbor retrieval. Our SPEAR with GRPO improves over the Search-R1 baseline on average, especially on the multi-hop QA benchmarks. Such multi-hop QA datasets require reasoning for problem decomposition and several turns of information seeking. In this case, our intrinsic reward that encourages multiple tool uses for broad exploration prevents arbitrary conclusions with only one or two searches. Our SPEAR respectively requires ~ 14.48 and ~ 14.42 calls for 7B and 14B models, respectively. Such behavior is expected due to the stimulation of exploration at the beginning. Despite the QA tasks are relatively short-horizon, the agent still benefits from the detailed decomposition of the complex queries with cross-validation via step-by-step searching. Note that our retrieval service adopts the HNSW E5 embedding for efficient training, which slightly impedes performance (Jin et al., 2025a).

5.6 MORE DISCUSSIONS

510 Due to the page limit, discussions on theoretical analysis on convergence A.9, hyper-
511 parameters A.13, qualitative analysis A.14, training cost and complexity A.15, and future research
512 directions A.16 are presented in the appendix. One could easily adapt SPEAR to training any
513 (M)LLM-driven agents robustly without binding to a specific optimization algorithm.

516 6 CONCLUSIONS AND LIMITATIONS

518 In this paper, we target the pivotal challenge of balancing exploration and exploitation in RL training
519 of LLM agents. Our proposed solution, SPEAR , extends the vanilla SIL by advantage recalibration,
520 scheduled entropy control, and intrinsic rewards. These components work in a curriculum manner
521 to prevent policy collapse and excessive uncertainty, progressively guiding the policy through
522 a smooth transition between exploration and exploitation. In addition, we propose a strong base-
523 line *Dr:BoT* tailored for agentic RL with existing bag-of-tricks verified from numerical industrial
524 practices. Empirical results across tasks and models showcase SPEAR’s superiority over existing
525 methods, with performance boosts and acceptable computational overhead. The effectiveness of our
526 SPEAR underscores the value of learning from past experiences while managing policy entropy,
527 offering a robust framework for training LLMs with strong reasoning and tool integration skills.

528 There exist two potential limitations: 1) The vague definition of good experiences under highly
529 complex, stochastic environments with unreliable tools. In such cases, observations can be noisy
530 and severely degrade the feasibility of the task. The sparse outcome reward cannot distinguish
531 between good and bad experiences and thereafter the relative advantages might be simply attributed
532 to randomness instead of the agent’s behavior. We suggest a possible solution that more fine-grained,
533 stepwise supervision should be enforced. For example, a step-wise process reward that evaluates the
534 logical consistency (Zhang et al., 2025b) of the agent’s thought and action might be helpful. 2) The
535 rigidity of entropy control which relies on prior-based scheduling and covariance-based clipping. In
536 the present study, the proposed scheduling and clipping designs might not be optimal for all kinds of
537 agentic tasks. A more adaptive solution lies in the policy’s self-confidence on decisions under each
538 observation. One might use the token-level dynamic reweighting for SIL (Wu et al., 2025) which
539 avoids over-concentration on certain low-probability reference tokens in the replay buffer. Similarly,
the clipping could depend on token probability instead of the bounded random sampling. We leave
the exploration mentioned above as a promising direction for improvement in the future.

540 **Ethics Statement.** The present study conforms with the ICLR Code of Ethics. The paper does not
 541 involve crowdsourcing nor research with human subjects.
 542

543 **Reproducibility Statement.** All datasets used in the paper are publicly accessible (see Sec-
 544 tion 5.1). All the codes are available at [https://anonymous.4open.science/r/SPEAR_](https://anonymous.4open.science/r/SPEAR_anonymous-2104/README.md)
 545 anonymous-2104/README.md for reproduction. In addition, we provide all the details of im-
 546 plementation in Section A.12.
 547

548 **REFERENCES**
 549

550 Josh Achiam, Steven Adler, Sandhini Agarwal, Lama Ahmad, Ilge Akkaya, Florencia Leoni Ale-
 551 man, Diogo Almeida, Janko Altenschmidt, Sam Altman, Shyamal Anadkat, et al. Gpt-4 technical
 552 report. *arXiv preprint arXiv:2303.08774*, 2023.

553 Shipra Agrawal and Navin Goyal. Analysis of thompson sampling for the multi-armed bandit prob-
 554 lem. In *Conference on learning theory*, pp. 39–1. JMLR Workshop and Conference Proceedings,
 555 2012.

556 Arash Ahmadian, Chris Cremer, Matthias Gallé, Marzieh Fadaee, Julia Kreutzer, Olivier Pietquin,
 557 Ahmet Üstün, and Sara Hooker. Back to basics: Revisiting reinforce style optimization for learn-
 558 ing from human feedback in llms. *arXiv preprint arXiv:2402.14740*, 2024.

559 AIME. Aime problems and solutions. https://artofproblemsolving.com/wiki/index.php/AIME_Problems_and_Solutions, 2025.

560 Fei Bai, Yingqian Min, Beichen Zhang, Zhipeng Chen, Wayne Xin Zhao, Lei Fang, Zheng Liu,
 561 Zhongyuan Wang, and Ji-Rong Wen. Towards effective code-integrated reasoning. *arXiv preprint*
 562 *arXiv:2505.24480*, 2025a.

563 Shuai Bai, Keqin Chen, Xuejing Liu, Jialin Wang, Wenbin Ge, Sibo Song, Kai Dang, Peng Wang,
 564 Shijie Wang, Jun Tang, et al. Qwen2. 5-vl technical report. *arXiv preprint arXiv:2502.13923*,
 565 2025b.

566 Marc Bellemare, Sriram Srinivasan, Georg Ostrovski, Tom Schaul, David Saxton, and Remi Munos.
 567 Unifying count-based exploration and intrinsic motivation. *Advances in neural information pro-*
 568 *cessing systems*, 29, 2016.

569 Bytedance-Seed-Foundation-Code-Team, :, Yao Cheng, Jianfeng Chen, Jie Chen, Li Chen, Liyu
 570 Chen, Wentao Chen, Zhengyu Chen, Shijie Geng, Aoyan Li, Bo Li, Bowen Li, Linyi Li, Boyi
 571 Liu, Jiaheng Liu, Kaibo Liu, Qi Liu, Shukai Liu, Siyao Liu, Tianyi Liu, Tingkai Liu, Yongfei Liu,
 572 Rui Long, Jing Mai, Guanghan Ning, Z. Y. Peng, Kai Shen, Jiahao Su, Jing Su, Tao Sun, Yifan
 573 Sun, Yunzhe Tao, Guoyin Wang, Siwei Wang, Xuwu Wang, Yite Wang, Zihan Wang, Jinxiang
 574 Xia, Liang Xiang, Xia Xiao, Yongsheng Xiao, Chenguang Xi, Shulin Xin, Jingjing Xu, Shikun
 575 Xu, Hongxia Yang, Jack Yang, Yingxiang Yang, Jianbo Yuan, Jun Zhang, Yufeng Zhang, Yuyu
 576 Zhang, Shen Zheng, He Zhu, and Ming Zhu. Fullstack bench: Evaluating llms as full stack coders,
 577 2025. URL <https://arxiv.org/abs/2412.00535>.

578 Paul F Christiano, Jan Leike, Tom Brown, Miljan Martic, Shane Legg, and Dario Amodei. Deep
 579 reinforcement learning from human preferences. *Advances in neural information processing sys-*
 580 *tems*, 30, 2017.

581 Marc-Alexandre Côté, Akos Kádár, Xingdi Yuan, Ben Kybartas, Tavian Barnes, Emery Fine, James
 582 Moore, Matthew Hausknecht, Layla El Asri, Mahmoud Adada, et al. Textworld: A learning
 583 environment for text-based games. In *Workshop on Computer Games*, pp. 41–75. Springer, 2018.

584 Ganqu Cui, Lifan Yuan, Zefan Wang, Hanbin Wang, Yuchen Zhang, Jiacheng Chen, Wendi Li,
 585 Bingxiang He, Yuchen Fan, Tianyu Yu, et al. Process reinforcement through implicit rewards.
 586 *arXiv preprint arXiv:2502.01456*, 2025a.

587 Ganqu Cui, Yuchen Zhang, Jiacheng Chen, Lifan Yuan, Zhi Wang, Yuxin Zuo, Haozhan Li, Yuchen
 588 Fan, Huayu Chen, Weize Chen, et al. The entropy mechanism of reinforcement learning for
 589 reasoning language models. *arXiv preprint arXiv:2505.22617*, 2025b.

594 Jeff Da, Clinton Wang, Xiang Deng, Yuntao Ma, Nikhil Barhate, and Sean Hendryx. Agent-rlvr:
 595 Training software engineering agents via guidance and environment rewards. *arXiv preprint*
 596 *arXiv:2506.11425*, 2025.

597 Thomas Degrif, Martha White, and Richard S Sutton. Off-policy actor-critic. *arXiv preprint*
 598 *arXiv:1205.4839*, 2012.

599 Wenlong Deng, Yi Ren, Muchen Li, Danica J Sutherland, Xiaoxiao Li, and Christos Thrampoulidis.
 600 On the effect of negative gradient in group relative deep reinforcement optimization. *arXiv*
 601 *preprint arXiv:2505.18830*, 2025.

602 Guanting Dong, Yifei Chen, Xiaoxi Li, Jiajie Jin, Hongjin Qian, Yutao Zhu, Hangyu Mao, Guorui
 603 Zhou, Zhicheng Dou, and Ji-Rong Wen. Tool-star: Empowering llm-brained multi-tool reasoner
 604 via reinforcement learning. *arXiv preprint arXiv:2505.16410*, 2025a.

605 Guanting Dong, Hangyu Mao, Kai Ma, Licheng Bao, Yifei Chen, Zhongyuan Wang, Zhongxia
 606 Chen, Jiazen Du, Huiyang Wang, Fuzheng Zhang, et al. Agentic reinforced policy optimization.
 607 *arXiv preprint arXiv:2507.19849*, 2025b.

608 Benjamin Eysenbach, Abhishek Gupta, Julian Ibarz, and Sergey Levine. Diversity is all you need:
 609 Learning skills without a reward function. *arXiv preprint arXiv:1802.06070*, 2018.

610 Jiazhan Feng, Shijue Huang, Xingwei Qu, Ge Zhang, Yujia Qin, Baoquan Zhong, Chengquan Jiang,
 611 Jinxin Chi, and Wanjun Zhong. Retool: Reinforcement learning for strategic tool use in llms.
 612 *arXiv preprint arXiv:2504.11536*, 2025a.

613 Lang Feng, Zhenghai Xue, Tingcong Liu, and Bo An. Group-in-group policy optimization for llm
 614 agent training. *arXiv preprint arXiv:2505.10978*, 2025b.

615 Johan Ferret, Olivier Pietquin, and Matthieu Geist. Self-imitation advantage learning. *arXiv preprint*
 616 *arXiv:2012.11989*, 2020.

617 Hiroki Furuta, Kuang-Huei Lee, Ofir Nachum, Yutaka Matsuo, Aleksandra Faust, Shixiang Shane
 618 Gu, and Izzeddin Gur. Multimodal web navigation with instruction-finetuned foundation models.
 619 *arXiv preprint arXiv:2305.11854*, 2023.

620 Tanmay Gangwani, Qiang Liu, and Jian Peng. Learning self-imitating diverse policies. *arXiv*
 621 *preprint arXiv:1805.10309*, 2018.

622 Jiaxuan Gao, Wei Fu, Minyang Xie, Shusheng Xu, Chuyi He, Zhiyu Mei, Banghua Zhu, and Yi Wu.
 623 Beyond ten turns: Unlocking long-horizon agentic search with large-scale asynchronous rl. *arXiv*
 624 *preprint arXiv:2508.07976*, 2025.

625 Zhibin Gou, Zhihong Shao, Yeyun Gong, Yelong Shen, Yujiu Yang, Minlie Huang, Nan Duan, and
 626 Weizhu Chen. Tora: A tool-integrated reasoning agent for mathematical problem solving. *arXiv*
 627 *preprint arXiv:2309.17452*, 2023.

628 Karol Gregor, Danilo Jimenez Rezende, and Daan Wierstra. Variational intrinsic control. *arXiv*
 629 *preprint arXiv:1611.07507*, 2016.

630 Yu Gu, Kai Zhang, Yuting Ning, Boyuan Zheng, Boyu Gou, Tianci Xue, Cheng Chang, Sanjari
 631 Srivastava, Yanan Xie, Peng Qi, et al. Is your llm secretly a world model of the internet? model-
 632 based planning for web agents. *arXiv preprint arXiv:2411.06559*, 2024.

633 Daya Guo, Dejian Yang, Haowei Zhang, Junxiao Song, Ruoyu Zhang, Runxin Xu, Qihao Zhu,
 634 Shirong Ma, Peiyi Wang, Xiao Bi, et al. Deepseek-rl: Incentivizing reasoning capability in llms
 635 via reinforcement learning. *arXiv preprint arXiv:2501.12948*, 2025.

636 Tuomas Haarnoja, Haoran Tang, Pieter Abbeel, and Sergey Levine. Reinforcement learning with
 637 deep energy-based policies. In *International conference on machine learning*, pp. 1352–1361.
 638 PMLR, 2017.

639 Tuomas Haarnoja, Aurick Zhou, Pieter Abbeel, and Sergey Levine. Soft actor-critic: Off-policy
 640 maximum entropy deep reinforcement learning with a stochastic actor. In *International confer-
 641 ence on machine learning*, pp. 1861–1870. Pmlr, 2018.

648 Jianye Hao, Tianpei Yang, Hongyao Tang, Chenjia Bai, Jinyi Liu, Zhaopeng Meng, Peng Liu, and
 649 Zhen Wang. Exploration in deep reinforcement learning: From single-agent to multiagent domain.
 650 *IEEE Transactions on Neural Networks and Learning Systems*, 35(7):8762–8782, 2023.

651

652 Alex Havrilla, Yuqing Du, Sharath Chandra Raparthy, Christoforos Nalmpantis, Jane Dwivedi-Yu,
 653 Maksym Zhuravinskyi, Eric Hambro, Sainbayar Sukhbaatar, and Roberta Raileanu. Teaching
 654 large language models to reason with reinforcement learning. *arXiv preprint arXiv:2403.04642*,
 655 2024.

656 Hongliang He, Wenlin Yao, Kaixin Ma, Wenhao Yu, Yong Dai, Hongming Zhang, Zhenzhong Lan,
 657 and Dong Yu. Webvoyager: Building an end-to-end web agent with large multimodal models.
 658 *arXiv preprint arXiv:2401.13919*, 2024.

659 Xanh Ho, Anh-Khoa Duong Nguyen, Saku Sugawara, and Akiko Aizawa. Constructing a multi-hop
 660 qa dataset for comprehensive evaluation of reasoning steps. *arXiv preprint arXiv:2011.01060*,
 661 2020.

662

663 Wenyi Hong, Weihan Wang, Qingsong Lv, Jiazheng Xu, Wenmeng Yu, Junhui Ji, Yan Wang, Zihan
 664 Wang, Yuxiao Dong, Ming Ding, et al. Cogagent: A visual language model for gui agents.
 665 In *Proceedings of the IEEE/CVF Conference on Computer Vision and Pattern Recognition*, pp.
 666 14281–14290, 2024.

667 Dan Horgan, John Quan, David Budden, Gabriel Barth-Maron, Matteo Hessel, Hado Van Hasselt,
 668 and David Silver. Distributed prioritized experience replay. *arXiv preprint arXiv:1803.00933*,
 669 2018.

670 Rein Houthooft, Xi Chen, Yan Duan, John Schulman, Filip De Turck, and Pieter Abbeel. Vime:
 671 Variational information maximizing exploration. *Advances in neural information processing sys-
 672 tems*, 29, 2016.

673

674 Peter J Huber. Robust statistics. In *International encyclopedia of statistical science*, pp. 1248–1251.
 675 Springer, 2011.

676

677 Aaron Jaech, Adam Kalai, Adam Lerer, Adam Richardson, Ahmed El-Kishky, Aiden Low, Alec
 678 Helyar, Aleksander Madry, Alex Beutel, Alex Carney, et al. Openai o1 system card. *arXiv
 679 preprint arXiv:2412.16720*, 2024.

680

681 Bowen Jin, Jinsung Yoon, Priyanka Kargupta, Sercan O Arik, and Jiawei Han. An empirical
 682 study on reinforcement learning for reasoning-search interleaved llm agents. *arXiv preprint
 683 arXiv:2505.15117*, 2025a.

684

685 Bowen Jin, Hansi Zeng, Zhenrui Yue, Jinsung Yoon, Sercan Arik, Dong Wang, Hamed Zamani, and
 686 Jiawei Han. Search-r1: Training llms to reason and leverage search engines with reinforcement
 687 learning. *arXiv preprint arXiv:2503.09516*, 2025b.

688

689 Mandar Joshi, Eunsol Choi, Daniel S Weld, and Luke Zettlemoyer. Triviaqa: A large scale distantly
 690 supervised challenge dataset for reading comprehension. *arXiv preprint arXiv:1705.03551*, 2017.

691

692 Woojun Kim and Youngchul Sung. An adaptive entropy-regularization framework for multi-agent
 693 reinforcement learning. In *International Conference on Machine Learning*, pp. 16829–16852.
 694 PMLR, 2023.

695

696 Wouter Kool, Herke van Hoof, and Max Welling. Buy 4 reinforce samples, get a baseline for free!
 697 2019.

698

699 Tom Kwiatkowski, Jennimaria Palomaki, Olivia Redfield, Michael Collins, Ankur Parikh, Chris
 700 Alberti, Danielle Epstein, Illia Polosukhin, Jacob Devlin, Kenton Lee, et al. Natural questions: a
 701 benchmark for question answering research. *Transactions of the Association for Computational
 702 Linguistics*, 7:453–466, 2019.

702

703 Woosuk Kwon, Zhuohan Li, Siyuan Zhuang, Ying Sheng, Lianmin Zheng, Cody Hao Yu, Joseph E.
 704 Gonzalez, Hao Zhang, and Ion Stoica. Efficient memory management for large language model
 705 serving with pagedattention. In *Proceedings of the ACM SIGOPS 29th Symposium on Operating
 706 Systems Principles*, 2023.

702 Paweł Ladosz, Lilian Weng, Minwoo Kim, and Hyondong Oh. Exploration in deep reinforcement
 703 learning: A survey. *Information Fusion*, 85:1–22, 2022.

704

705 Nathan Lambert, Jacob Morrison, Valentina Pyatkin, Shengyi Huang, Hamish Ivison, Faeze Brah-
 706 man, Lester James V Miranda, Alisa Liu, Nouha Dziri, Shane Lyu, et al. Tulu 3: Pushing frontiers
 707 in open language model post-training. *arXiv preprint arXiv:2411.15124*, 2024.

708

709 John Law. Robust statistics—the approach based on influence functions, 1986.

710

711 Lei Li, Yekun Chai, Shuohuan Wang, Yu Sun, Hao Tian, Ningyu Zhang, and Hua Wu. Tool-
 712 augmented reward modeling. *arXiv preprint arXiv:2310.01045*, 2023.

713

714 Manling Li, Shiyu Zhao, Qineng Wang, Kangrui Wang, Yu Zhou, Sanjana Srivastava, Cem Gokmen,
 715 Tony Lee, Erran Li Li, Ruohan Zhang, et al. Embodied agent interface: Benchmarking llms for
 716 embodied decision making. *Advances in Neural Information Processing Systems*, 37:100428–
 100534, 2024.

717

718 Ning Li, Xiangmou Qu, Jiamu Zhou, Jun Wang, Muning Wen, Kounianhua Du, Xingyu Lou, Qiuy-
 719 ing Peng, and Weinan Zhang. Mobileuse: A gui agent with hierarchical reflection for autonomous
 720 mobile operation. *arXiv preprint arXiv:2507.16853*, 2025a.

721

722 Weizhen Li, Jianbo Lin, Zhusong Jiang, Jingyi Cao, Xinpeng Liu, Jiayu Zhang, Zhenqiang Huang,
 723 Qianben Chen, Weichen Sun, Qixiang Wang, et al. Chain-of-agents: End-to-end agent founda-
 724 tion models via multi-agent distillation and agentic rl. *arXiv preprint arXiv:2508.13167*, 2025b.

725

726 Xiaoxi Li, Jiajie Jin, Guanting Dong, Hongjin Qian, Yutao Zhu, Yongkang Wu, Ji-Rong Wen, and
 727 Zhicheng Dou. Webthinker: Empowering large reasoning models with deep research capability.
 728 *arXiv preprint arXiv:2504.21776*, 2025c.

729

730 Xuefeng Li, Haoyang Zou, and Pengfei Liu. Torl: Scaling tool-integrated rl. *arXiv preprint
 731 arXiv:2503.23383*, 2025d.

732

733 Heng Lin and Zhongwen Xu. Understanding tool-integrated reasoning. *arXiv preprint
 734 arXiv:2508.19201*, 2025.

735

736 Xiaoqian Liu, Ke Wang, Yuchuan Wu, Fei Huang, Yongbin Li, Junge Zhang, and Jianbin Jiao.
 737 Agentic reinforcement learning with implicit step rewards. *arXiv preprint arXiv:2509.19199*,
 738 2025a.

739

740 Zichen Liu, Changyu Chen, Wenjun Li, Penghui Qi, Tianyu Pang, Chao Du, Wee Sun Lee,
 741 and Min Lin. Understanding rl-zero-like training: A critical perspective. *arXiv preprint
 742 arXiv:2503.20783*, 2025b.

743

744 Zihe Liu, Jiashun Liu, Yancheng He, Weixun Wang, Jiaheng Liu, Ling Pan, Xinyu Hu, Shaopan
 745 Xiong, Ju Huang, Jian Hu, et al. Part i: Tricks or traps? a deep dive into rl for llm reasoning.
 746 *arXiv preprint arXiv:2508.08221*, 2025c.

747

748 Xinji Mai, Haotian Xu, Weinong Wang, Jian Hu, Yingying Zhang, Wenqiang Zhang, et al. Agent rl
 749 scaling law: Agent rl with spontaneous code execution for mathematical problem solving. *arXiv
 750 preprint arXiv:2505.07773*, 2025.

751

752 Alex Mallen, Akari Asai, Victor Zhong, Rajarshi Das, Daniel Khashabi, and Hannaneh Hajishirzi.
 753 When not to trust language models: Investigating effectiveness of parametric and non-parametric
 754 memories. In *Proceedings of the 61st Annual Meeting of the Association for Computational
 755 Linguistics (Volume 1: Long Papers)*, pp. 9802–9822, 2023.

756

757 Negar Mehr, Mingyu Wang, Maulik Bhatt, and Mac Schwager. Maximum-entropy multi-agent
 758 dynamic games: Forward and inverse solutions. *IEEE transactions on robotics*, 39(3):1801–1815,
 759 2023.

756 Thomas M Moerland, Joost Broekens, Aske Plaat, Catholijn M Jonker, et al. Model-based rein-
 757 force learning: A survey. *Foundations and Trends® in Machine Learning*, 16(1):1–118,
 758 2023.

759

760 Niklas Muennighoff, Zitong Yang, Weijia Shi, Xiang Lisa Li, Li Fei-Fei, Hannaneh Hajishirzi, Luke
 761 Zettlemoyer, Percy Liang, Emmanuel Candès, and Tatsunori Hashimoto. s1: Simple test-time
 762 scaling. *arXiv preprint arXiv:2501.19393*, 2025.

763 Junhyuk Oh, Yijie Guo, Satinder Singh, and Honglak Lee. Self-imitation learning. In *International
 764 conference on machine learning*, pp. 3878–3887. PMLR, 2018.

765

766 Long Ouyang, Jeffrey Wu, Xu Jiang, Diogo Almeida, Carroll Wainwright, Pamela Mishkin, Chong
 767 Zhang, Sandhini Agarwal, Katarina Slama, Alex Ray, et al. Training language models to fol-
 768 low instructions with human feedback. *Advances in neural information processing systems*, 35:
 769 27730–27744, 2022.

770 Yangchen Pan, Jincheng Mei, Amir-massoud Farahmand, Martha White, Hengshuai Yao, Mohsen
 771 Rohani, and Jun Luo. Understanding and mitigating the limitations of prioritized experience
 772 replay. In *Uncertainty in Artificial Intelligence*, pp. 1561–1571. PMLR, 2022.

773

774 Deepak Pathak, Pulkit Agrawal, Alexei A Efros, and Trevor Darrell. Curiosity-driven exploration
 775 by self-supervised prediction. In *International conference on machine learning*, pp. 2778–2787.
 776 PMLR, 2017.

777 Ofir Press, Muru Zhang, Sewon Min, Ludwig Schmidt, Noah A Smith, and Mike Lewis. Measuring
 778 and narrowing the compositionality gap in language models. In *Findings of the Association for
 779 Computational Linguistics: EMNLP 2023*, pp. 5687–5711, 2023.

780 Georgiy Pshikhachev, Dmitry Ivanov, Vladimir Egorov, and Aleksei Shpilman. Self-imitation learn-
 781 ing from demonstrations. *arXiv preprint arXiv:2203.10905*, 2022.

782

783 Cheng Qian, Emre Can Acikgoz, Qi He, Hongru Wang, Xiusi Chen, Dilek Hakkani-Tür, Gokhan
 784 Tur, and Heng Ji. Toolrl: Reward is all tool learning needs. *arXiv preprint arXiv:2504.13958*,
 785 2025.

786 Yujia Qin, Yining Ye, Junjie Fang, Haoming Wang, Shihao Liang, Shizuo Tian, Junda Zhang, Jiahao
 787 Li, Yunxin Li, Shijue Huang, et al. Ui-tars: Pioneering automated gui interaction with native
 788 agents. *arXiv preprint arXiv:2501.12326*, 2025a.

789

790 Yulei Qin, Gang Li, Zongyi Li, Zihan Xu, Yuchen Shi, Zhekai Lin, Xiao Cui, Ke Li, and Xing
 791 Sun. Incentivizing reasoning for advanced instruction-following of large language models. *arXiv
 792 preprint arXiv:2506.01413*, 2025b.

793

794 Yulei Qin, Yuncheng Yang, Pengcheng Guo, Gang Li, Hang Shao, Yuchen Shi, Zihan Xu, Yun Gu,
 795 Ke Li, and Xing Sun. Unleashing the power of data tsunami: A comprehensive survey on data
 796 assessment and selection for instruction tuning of language models. *Transactions on Machine
 797 Learning Research*, 2025c.

798

799 Baturay Saglam, Furkan B Mutlu, Dogan C Cicek, and Suleyman S Kozat. Actor prioritized expe-
 800 rience replay. *Journal of Artificial Intelligence Research*, 78:639–672, 2023.

801

802 Tom Schaul, John Quan, Ioannis Antonoglou, and David Silver. Prioritized experience replay. *arXiv
 803 preprint arXiv:1511.05952*, 2015.

804

805 Max-Philipp B. Schrader. gym-sokoban. [https://github.com/mpSchrader/
 806 gym-sokoban](https://github.com/mpSchrader/gym-sokoban), 2018.

807

808 John Schulman, Philipp Moritz, Sergey Levine, Michael Jordan, and Pieter Abbeel. High-
 809 dimensional continuous control using generalized advantage estimation. *arXiv preprint
 810 arXiv:1506.02438*, 2015.

811

812 John Schulman, Xi Chen, and Pieter Abbeel. Equivalence between policy gradients and soft q-
 813 learning. *arXiv preprint arXiv:1704.06440*, 2017a.

810 John Schulman, Filip Wolski, Prafulla Dhariwal, Alec Radford, and Oleg Klimov. Proximal policy
 811 optimization algorithms. *arXiv preprint arXiv:1707.06347*, 2017b.
 812

813 Younggyo Seo, Lili Chen, Jinwoo Shin, Honglak Lee, Pieter Abbeel, and Kimin Lee. State entropy
 814 maximization with random encoders for efficient exploration. In *International conference on
 815 machine learning*, pp. 9443–9454. PMLR, 2021.

816 Zhihong Shao, Peiyi Wang, Qihao Zhu, Runxin Xu, Junxiao Song, Xiao Bi, Haowei Zhang,
 817 Mingchuan Zhang, YK Li, Yang Wu, et al. Deepseekmath: Pushing the limits of mathemati-
 818 cal reasoning in open language models. *arXiv preprint arXiv:2402.03300*, 2024.
 819

820 Guangming Sheng, Chi Zhang, Zilingfeng Ye, Xibin Wu, Wang Zhang, Ru Zhang, Yanghua Peng,
 821 Haibin Lin, and Chuan Wu. Hybridflow: A flexible and efficient rlhf framework. *arXiv preprint
 822 arXiv: 2409.19256*, 2024.

823 Noah Shinn, Federico Cassano, Ashwin Gopinath, Karthik Narasimhan, and Shunyu Yao. Reflexion:
 824 Language agents with verbal reinforcement learning. *Advances in Neural Information Processing
 825 Systems*, 36:8634–8652, 2023.

826 Mohit Shridhar, Xingdi Yuan, Marc-Alexandre Côté, Yonatan Bisk, Adam Trischler, and Matthew
 827 Hausknecht. Alfworld: Aligning text and embodied environments for interactive learning. *arXiv
 828 preprint arXiv:2010.03768*, 2020.
 829

830 Joykirat Singh, Raghav Magazine, Yash Pandya, and Akshay Nambi. Agentic reasoning and tool
 831 integration for llms via reinforcement learning. *arXiv preprint arXiv:2505.01441*, 2025.

832 Jasper Snoek, Hugo Larochelle, and Ryan P Adams. Practical bayesian optimization of machine
 833 learning algorithms. *Advances in neural information processing systems*, 25, 2012.
 834

835 Xingwu Sun, Yanfeng Chen, Yiqing Huang, Ruobing Xie, Jiaqi Zhu, Kai Zhang, Shuaipeng Li,
 836 Zhen Yang, Jonny Han, Xiaobo Shu, et al. Hunyuan-large: An open-source moe model with 52
 837 billion activated parameters by tencent. *arXiv preprint arXiv:2411.02265*, 2024.

838 Zetian Sun, Dongfang Li, Zhuoer Chen, Yuhuai Qin, and Baotian Hu. Stabilizing long-term multi-
 839 turn reinforcement learning with gated rewards. *arXiv preprint arXiv:2508.10548*, 2025.
 840

841 Richard S Sutton. Learning to predict by the methods of temporal differences. *Machine learning*, 3
 842 (1):9–44, 1988.
 843

844 Richard S Sutton, Andrew G Barto, et al. *Reinforcement learning: An introduction*, volume 1. MIT
 845 press Cambridge, 1998.
 846

847 Haoran Tang, Rein Houthooft, Davis Foote, Adam Stooke, OpenAI Xi Chen, Yan Duan, John Schul-
 848 man, Filip DeTurck, and Pieter Abbeel. # exploration: A study of count-based exploration for
 849 deep reinforcement learning. *Advances in neural information processing systems*, 30, 2017.
 850

851 Yunhao Tang. Self-imitation learning via generalized lower bound q-learning. *Advances in neural
 852 information processing systems*, 33:13964–13975, 2020.
 853

854 Zhengwei Tao, Jialong Wu, Wenbiao Yin, Junkai Zhang, Baixuan Li, Haiyang Shen, Kuan Li,
 855 Liwen Zhang, Xinyu Wang, Yong Jiang, et al. Webshaper: Agentically data synthesizing via
 856 information-seeking formalization. *arXiv preprint arXiv:2507.15061*, 2025.
 857

858 Gemini Team, Rohan Anil, Sebastian Borgeaud, Jean-Baptiste Alayrac, Jiahui Yu, Radu Soricut,
 859 Johan Schalkwyk, Andrew M Dai, Anja Hauth, Katie Millican, et al. Gemini: a family of highly
 860 capable multimodal models. *arXiv preprint arXiv:2312.11805*, 2023.
 861

862 NovaSky Team. Sky-t1: Train your own o1 preview model within \$450, 2025a.
 863

864 Qwen Team. Qwq-32b: Embracing the power of reinforcement learning, 2025b.
 865

866 Harsh Trivedi, Niranjan Balasubramanian, Tushar Khot, and Ashish Sabharwal. Musique: Multihop
 867 questions via single-hop question composition. *Transactions of the Association for Computational
 868 Linguistics*, 10:539–554, 2022.

864 Haoran Wang, Thaleia Zariphopoulou, and Xunyu Zhou. Exploration versus exploitation in rein-
 865 forcement learning: A stochastic control approach. *arXiv preprint arXiv:1812.01552*, 2018.
 866

867 Junyang Wang, Haiyang Xu, Haitao Jia, Xi Zhang, Ming Yan, Weizhou Shen, Ji Zhang, Fei Huang,
 868 and Jitao Sang. Mobile-agent-v2: Mobile device operation assistant with effective navigation via
 869 multi-agent collaboration. *Advances in Neural Information Processing Systems*, 37:2686–2710,
 870 2024.

871 Shenzhi Wang, Le Yu, Chang Gao, Chujie Zheng, Shixuan Liu, Rui Lu, Kai Dang, Xionghui Chen,
 872 Jianxin Yang, Zhenru Zhang, et al. Beyond the 80/20 rule: High-entropy minority tokens drive
 873 effective reinforcement learning for llm reasoning. *arXiv preprint arXiv:2506.01939*, 2025a.
 874

875 Zihan Wang, Kangrui Wang, Qineng Wang, Pingyue Zhang, Linjie Li, Zhengyuan Yang, Xing Jin,
 876 Kefan Yu, Minh Nhat Nguyen, Licheng Liu, et al. Ragen: Understanding self-evolution in llm
 877 agents via multi-turn reinforcement learning. *arXiv preprint arXiv:2504.20073*, 2025b.

878 Yifan Wei, Xiaoyan Yu, Yixuan Weng, Tengfei Pan, Angsheng Li, and Li Du. Autotir: Autonomous
 879 tools integrated reasoning via reinforcement learning. *arXiv preprint arXiv:2507.21836*, 2025.
 880

881 Ronald J Williams and Jing Peng. Function optimization using connectionist reinforcement learning
 882 algorithms. *Connection Science*, 3(3):241–268, 1991.
 883

884 Yongliang Wu, Yizhou Zhou, Zhou Ziheng, Yingzhe Peng, Xinyu Ye, Xinting Hu, Wenbo Zhu,
 885 Lu Qi, Ming-Hsuan Yang, and Xu Yang. On the generalization of sft: A reinforcement learning
 886 perspective with reward rectification. *arXiv preprint arXiv:2508.05629*, 2025.

887 Yu Xia, Jingru Fan, Weize Chen, Siyu Yan, Xin Cong, Zhong Zhang, Yaxi Lu, Yankai Lin, Zhiyuan
 888 Liu, and Maosong Sun. Agentrm: Enhancing agent generalization with reward modeling. *arXiv
 889 preprint arXiv:2502.18407*, 2025.
 890

891 Teng Xiao, Mingxiao Li, Yige Yuan, Huaisheng Zhu, Chao Cui, and Vasant G Honavar. How to
 892 leverage demonstration data in alignment for large language model? a self-imitation learning
 893 perspective. *arXiv preprint arXiv:2410.10093*, 2024.

894 Bo Xin, Haixu Yu, You Qin, Qing Tang, and Zhangqing Zhu. Exploration entropy for reinforcement
 895 learning. *Mathematical Problems in Engineering*, 2020(1):2672537, 2020.
 896

897 Zhenghai Xue, Longtao Zheng, Qian Liu, Yingru Li, Xiaosen Zheng, Zejun Ma, and Bo An. Sim-
 898 pletir: End-to-end reinforcement learning for multi-turn tool-integrated reasoning, 2025. URL
 899 <https://arxiv.org/abs/2509.02479>.

900 An Yang, Beichen Zhang, Binyuan Hui, Bofei Gao, Bowen Yu, Chengpeng Li, Dayiheng Liu, Jian-
 901 hong Tu, Jingren Zhou, Junyang Lin, et al. Qwen2. 5-math technical report: Toward mathematical
 902 expert model via self-improvement. *arXiv preprint arXiv:2409.12122*, 2024.
 903

904 An Yang, Anfeng Li, Baosong Yang, Beichen Zhang, Binyuan Hui, Bo Zheng, Bowen Yu,
 905 Chang Gao, Chengan Huang, Chenxu Lv, et al. Qwen3 technical report. *arXiv preprint
 906 arXiv:2505.09388*, 2025.
 907

908 Zhilin Yang, Peng Qi, Saizheng Zhang, Yoshua Bengio, William Cohen, Ruslan Salakhutdinov,
 909 and Christopher D Manning. Hotpotqa: A dataset for diverse, explainable multi-hop question
 910 answering. In *Proceedings of the 2018 conference on empirical methods in natural language
 911 processing*, pp. 2369–2380, 2018.

912 Feng Yao, Liyuan Liu, Dinghuai Zhang, Chengyu Dong, Jingbo Shang, and Jianfeng Gao. Your
 913 efficient rl framework secretly brings you off-policy rl training, August 2025. URL <https://fengyao.notion.site/off-policy-rl>.
 914

916 Shunyu Yao, Howard Chen, John Yang, and Karthik Narasimhan. Webshop: Towards scalable
 917 real-world web interaction with grounded language agents. *Advances in Neural Information Pro-
 918 cessing Systems*, 35:20744–20757, 2022.

918 Shunyu Yao, Jeffrey Zhao, Dian Yu, Nan Du, Izhak Shafran, Karthik Narasimhan, and Yuan Cao.
 919 React: Synergizing reasoning and acting in language models. In *International Conference on*
 920 *Learning Representations (ICLR)*, 2023.

921 Qiyi Yu, Zheng Zhang, Ruofei Zhu, Yufeng Yuan, Xiaochen Zuo, Yu Yue, Weinan Dai, Tiantian
 922 Fan, Gaohong Liu, Lingjun Liu, et al. Dapo: An open-source llm reinforcement learning system
 923 at scale. *arXiv preprint arXiv:2503.14476*, 2025.

924 Siliang Zeng, Quan Wei, William Brown, Oana Frunza, Yuriy Nevmyvaka, and Mingyi Hong. Re-
 925 infacing multi-turn reasoning in llm agents via turn-level credit assignment. *arXiv preprint*
 926 *arXiv:2505.11821*, 2025.

927 Chuheng Zhang, Yuanying Cai, Longbo Huang, and Jian Li. Exploration by maximizing rényi
 928 entropy for reward-free rl framework. In *Proceedings of the AAAI Conference on Artificial Intel-*
 929 *ligence*, volume 35, pp. 10859–10867, 2021.

930 Wenhao Zhang, Yuexiang Xie, Yuchang Sun, Yanxi Chen, Guoyin Wang, Yaliang Li, Bolin Ding,
 931 and Jingren Zhou. On-policy rl meets off-policy experts: Harmonizing supervised fine-tuning and
 932 reinforcement learning via dynamic weighting. *arXiv preprint arXiv:2508.11408*, 2025a.

933 Zijing Zhang, Ziyang Chen, Mingxiao Li, Zhaopeng Tu, and Xiaolong Li. Rlvmr: Reinforcement
 934 learning with verifiable meta-reasoning rewards for robust long-horizon agents. *arXiv preprint*
 935 *arXiv:2507.22844*, 2025b.

936 Rui Zhao, Xudong Sun, and Volker Tresp. Maximum entropy-regularized multi-goal reinforcement
 937 learning. In *International Conference on Machine Learning*, pp. 7553–7562. PMLR, 2019.

938 Richard Zhuang, Trung Vu, Alex Dimakis, and Maheswaran Sathiamoorthy. Improving multi-turn
 939 tool use with reinforcement learning. <https://www.bespokelabs.ai/blog/improving-multi-turn->
 940 tool-use-with-reinforcement-learning, 2025. Accessed: 2025-04-17.

941 Brian D Ziebart, Andrew L Maas, J Andrew Bagnell, Anind K Dey, et al. Maximum entropy inverse
 942 reinforcement learning. In *Aaai*, volume 8, pp. 1433–1438. Chicago, IL, USA, 2008.

943

944

945

946

947

948

949

950

951

952

953

954

955

956

957

958

959

960

961

962

963

964

965

966

967

968

969

970

971

972 **A APPENDIX**
973974 **A.1 SUMMARY OF THE APPENDIX**
975976 In the appendix, we provide detailed explanations on the following.
977978

- Descriptions about the Action Space
- Brief Introduction to the PPO and GRPO
- PseudoCode of the SPEAR
- Visualization of the Curriculum Schedule
- Definition of the Reward Function
- Descriptions about RL Bag-of-Tricks
- Theoretical Analysis on Convergence
- Descriptions of the Data and Environment
- Choice of Baselines
- Implementation Details
- Discussions and Guidelines on Hyper-parameters
- Qualitative Analysis
- Training Cost and Complexity
- Future Research Directions

998999 **A.2 DETAILED ACTION SPACE**
10001001 The following contents correspond to Section 3.1 in the main text.
10021003 **TextWorld Embodied Tool.** The embodied actions follows ALFWorld (Shridhar et al., 2020)
1004 where a language-driven agent interacts with the TextWorld (Côté et al., 2018). It allows the
1005 agent to take one of the following high-level actions: `goto {recep}`, `take {obj}` from
1006 `{recep}`, `put {obj}` in/on `{recep}`, `open {recep}`, `close {recep}`, `toggle`
1007 `{obj}{recep}`, `clean {obj}` with `{recep}`, `heat {obj}` with `{recep}`, and `cool`
1008 `{obj}` with `{recep}`, where `{obj}` and `{recep}` denote objects and receptacles, re-
1009 spectively.1010 **Web Browsing Tool.** The definition of web browsing follows WebShop (Yao et al., 2022)
1011 where only two actions are allowed: `search[query]` and `choose[button]` where `query`
1012 and `button` respectively stand for searching query and clickable elements such as back
1013 to search, prev/next page, `{product title}`, `{option}`, `{desc/overview}`,
1014 previous, and buy.1015 **Code Interpreter Tool.** The code interpreter executes the code generated by the language model
1016 and return both the `stdout` and `stderr`. If the code runs correctly, the `stdout` contains the
1017 output. On the other hand, the compiler error messages are provided for the next-round correc-
1018 tion. We follow (Feng et al., 2025a) to deploy a SandBox (Bytedance-Seed-Foundation-Code-Team
1019 et al., 2025) service that receives execution requests from the interpreter tool. In addition, we add
1020 a reminder in the `stdout` for empty output when the LLM forgets to print computation results:
1021 *Empty stdout! You might forget to print the answer.* For non-empty `stderr`, we also add an
1022 instruction as hint: *Errors occurred! Check your code.*1023 **A.3 DETAILED POLICY OPTIMIZATION ALGORITHMS**
1024

1025 The following contents correspond to Section 3.2 in the main text.

1026 **Proximal Policy Optimization (PPO).** Typically, PPO optimizes the following:
 1027

$$1028 \quad 1029 \quad 1030 \quad \mathcal{J}(\pi_\theta) = \mathbb{E}_{x \sim p(X), \mathbf{a} \sim \pi_\theta(\cdot|x, \mathbf{s})} \left[\mathcal{R}(x, \mathbf{s}, \mathbf{a}) - \beta D_{\text{KL}}[\pi_\theta(\cdot|x, \mathbf{s}) || \pi_{\text{ref}}(\cdot|x, \mathbf{s})] \right], \quad (7)$$

1031 where $\mathcal{R}(x, \mathbf{s}, \mathbf{a}) = \sum_{t=1}^T r_t(x, \mathbf{s}_t, \mathbf{a}_t)$ is the return (Sutton et al., 1998) for the trajectory and π_{ref}
 1032 is the reference policy model. The KL divergence proposed (Christiano et al., 2017) to prevent the
 1033 policy π_θ from deviating greatly from the reference π_{ref} ($\beta > 0$). In consideration of the simplicity,
 1034 we follow TULU 3 (Lambert et al., 2024) to adopt RL with the verifiable reward where the rule-
 1035 based verifiers are designed to provide the outcome reward signal r instead of the reward model r_θ .
 1036 In addition, we follow (Liu et al., 2025b) to drop the KL term by setting $\beta = 0$, which not only
 1037 emphasizes agent performance but also saves memory and computation during training.

1038 **Group Relative Policy Optimization (GRPO).** Specifically, the policy model $\pi_{\theta_{\text{old}}}$ from the pre-
 1039 vious iteration generates a group of G individual trajectories $\{\tau_i\}_{i=1}^G$. GRPO updates the policy π_θ
 1040 by maximizing the objective below.
 1041

$$1042 \quad 1043 \quad 1044 \quad \mathcal{J}_{\text{GRPO}}(\pi_\theta) = \mathbb{E}_{x \sim p(X), \{\tau_i\}_{i=1}^G \sim \pi_{\theta_{\text{old}}}(\cdot|x)} \frac{1}{G} \sum_{i=1}^G \mathcal{J}_{\text{GRPO}}^i, \quad (8)$$

$$1045 \quad \tau_i = \{(\mathbf{s}_1^i, \mathbf{a}_1^i, R_1^i), (\mathbf{s}_2^i, \mathbf{a}_2^i, R_2^i), \dots, (\mathbf{s}_T^i, \mathbf{a}_T^i, R_T^i)\},$$

$$1046 \quad 1047 \quad 1048 \quad \mathcal{J}_{\text{GRPO}}^i = \frac{1}{T} \sum_{t=1}^T \min \left[r_t^i(\theta) \hat{A}_t^i, \text{clip}[r_t^i(\theta), 1 - \epsilon, 1 + \epsilon] \hat{A}_t^i \right] - \beta D_{\text{KL}}^i(\pi_\theta || \pi_{\text{ref}}), \quad (9)$$

$$1049 \quad 1050 \quad 1051 \quad r_t^i = \frac{\pi_\theta(\mathbf{a}_t^i | x, \mathbf{s}_t^i)}{\pi_{\theta_{\text{old}}}(\mathbf{a}_t^i | x, \mathbf{s}_t^i)}, \hat{A}_t^i = \frac{R^i - \bar{R}}{\text{std}(\{R^i\}_{i=1}^G)}, \bar{R} = \text{mean}(\{R^i\}_{i=1}^G), \quad (10)$$

$$1052 \quad 1053 \quad 1054 \quad D_{\text{KL}}^i(\pi_\theta || \pi_{\text{ref}}) = \frac{\pi_{\text{ref}}(\mathbf{a}_t^i | x, \mathbf{s}_t^i)}{\pi_\theta(\mathbf{a}_t^i | x, \mathbf{s}_t^i)} - \log \frac{\pi_{\text{ref}}(\mathbf{a}_t^i | x, \mathbf{s}_t^i)}{\pi_\theta(\mathbf{a}_t^i | x, \mathbf{s}_t^i)} - 1. \quad (11)$$

1055 A.4 PSEUDO CODE

1056 The following contents correspond to Section 4 in the main text.

1057 Algorithm 1 summarizes the full training procedure of the proposed SPEAR. It is noted that our
 1058 SPEAR is compatible with various baselines such as GRPO (Shao et al., 2024) and GiGPO (Feng
 1059 et al., 2025b), enjoying a high-level of generalization. Specifically, the algorithm is featured by:
 1060 1) Maintenance of a replay buffer and a baseline buffer that respectively stores the trajectories for
 1061 good experience replay and estimates the current policy’s average performance; 2) Recalibration
 1062 of the previous advantages for off-policy update; 3) Regularization against the pre-mature entropy
 1063 collapsing; 4) Shaping of the composite intrinsic rewards for dominance of the outcome reward.

1064 Compared with the vanilla GRPO-like training, the proposed method only introduced: 1) Additional
 1065 policy update iterations positively associated with the number of N_D in terms of computational
 1066 complexity; 2) A replay buffer of the size N_D and a baseline performance buffer of the size N_{D_R} in
 1067 terms of space complexity.

1068 Since we re-utilize previous trajectories without completely re-computing the rollout generation,
 1069 log-probability estimation, and the advantages, such operations are light-weight and incur minimal
 1070 computation overhead. In the present study, we empirically set $N_D = 2048$ without meticulous
 1071 hyper-parameter tuning. For both ALFWorld, WebShop, and Sokoban, the number of trajectories per
 1072 data batch is the product of train_batch_size \times n_samples_per_prompt=256 and there exist around 4K
 1073 turn-level training samples under the VeRL-agent (Feng et al., 2025b) framework. For the DAPO-
 1074 MATH-17K, the number of trajectories per data batch is 2048 and there exist exactly 2048 trajectory-
 1075 level training samples under the VeRL (Sheng et al., 2024) framework. In this case, our replay buffer
 1076 reaches its full capacity around every two or three training steps on average for all experiments. For
 1077 each policy update by self-imitation, the number of iterations is comparable to that of the vanilla
 1078 policy update by GRPO under the present settings. The detailed analyses on the training cost and
 1079 complexity can also be found in Section A.15.

1080
1081
1082
1083

Algorithm 1 Training Agentic LLMs with SPEAR

Require: Initial policy $\pi_{\theta_{\text{old}}}$, data distribution $p(X)$, clipping bounds $\epsilon_{\text{lb}}, \epsilon_{\text{ub}}$, KL penalty β ($\beta = 0$), replay buffer \mathcal{D} with buffer size $N_{\mathcal{D}}$, intra-group baseline buffer \mathcal{D}_R with buffer size $N_{\mathcal{D}_R}$, the warm-up factor γ with the number of warm-up steps $T_{\text{warm-up}}$, covariance clipping bounds $\omega_{\text{lb}}, \omega_{\text{ub}}$, the covariance-based clipping ratio λ ($\lambda = 0.02$), the decay factor μ with the number of decay steps T_{decay} , the group size G , the maximum allowed interaction turns T .

Ensure: Updated policy π_{θ}

1: Initialize $\mathcal{D} = \emptyset$ and $\mathcal{D}_R = \emptyset$

2: **for** each training step t_{iter} **do**

3: Update the old policy model: $\theta_{\text{old}} \leftarrow \theta$

4: **# Repeat batch sampling and rollout generation for trajectories**

5: Sample data batch with each unique sample $x \sim p(X)$

6: **# Sample G trajectories $\{\tau_i\}_{i=1}^G$ for each x**

7: **for** $i = 1$ to G **do**

8: Initialize environment states \mathbf{s}_1^i

9: **# Sample at most T actions**

10: **for** $t = 1$ to T **do**

11: Sample action $\mathbf{a}_t^i \sim \pi_{\theta}(\cdot | x, \mathbf{s}_t^i)$

12: Execute actions, receive rewards R_t^i , observe the new states \mathbf{s}_{t+1}^i

13: **end for**

14: Organize the trajectory $\tau_i = \{(\mathbf{s}_1^i, \mathbf{a}_1^i, R_1^i), (\mathbf{s}_2^i, \mathbf{a}_2^i, R_2^i), \dots, (\mathbf{s}_T^i, \mathbf{a}_T^i, R_T^i)\}$

15: **end for**

16: **# Apply intrinsic reward shaping for advantage estimation**

17: Compute the vanilla objective $\mathcal{J}_{\text{GRPO}}(\pi_{\theta})$ via Equation 8 with the decay-scheduled R^i via Equation 6

18: **# Maintain the replay buffer and the baseline buffer**

19: $\mathcal{D}_R \leftarrow \mathcal{D}_R \cup \{\bar{R}\}, \bar{R} = \text{mean}(\{R^i\}_{i=1}^G)$

20: **while** $|\mathcal{D}_R| > N_{\mathcal{D}_R}$ **do**

21: Pop the oldest baseline $\mathcal{D}_R \leftarrow \mathcal{D}_R \setminus \{\bar{R}_0\}$

22: **end while**

23: **if** $|\mathcal{D}| < N_{\mathcal{D}}$ **then**

24: **# Add trajectories into the buffer only when their advantages are positive**

25: $\mathcal{D} \leftarrow \mathcal{D} \cup \{\tau_i | \hat{A}_i > 0\}$

26: **# Apply on-Policy update with the vanilla GRPO**

27: Update policy by maximizing objective $\mathcal{J}_{\text{GRPO}}(\pi_{\theta})$

28: **else**

29: **# Recalibrate the advantage**

30: Compute the newly estimated advantage \tilde{A}_j for all $\tau_j \in \mathcal{D}$ via Equation 2

31: Only keep τ_j with positive \tilde{A}_j as $\mathcal{D} \leftarrow \{\tau_j | \tilde{A}_j > 0, \forall \tau_j \in \mathcal{D}\}$

32: **# Apply regularization on self-imitation learning**

33: Compute the self-imitation objective $\tilde{\mathcal{J}}_{\text{GRPO}}^{\text{SIL-R}}(\pi_{\theta})$ via Equation 18 with covariance-based clipping via Equation 19

34: Apply the warm-up schedule for the total objective $\mathcal{J}_{\text{Total}}(\pi_{\theta})$ via Equation 5

35: **# Apply both the on-policy and the off-policy update for self-imitation**

36: Update policy by maximizing objective $\mathcal{J}_{\text{Total}}(\pi_{\theta})$

37: Reset the replay buffer $\mathcal{D} \leftarrow \emptyset$

38: **end if**

39: **end for**

40: **return** π_{θ}

1130
1131
1132
1133

1134 A.5 POLICY ENTROPY
11351136 The following contents are mentioned in Section 4.2 in the main text.
11371138 The policy entropy quantifies the confidence inherent in the actions triggered off by the LLM. Under
1139 the context of agent tasks, we measure the average entropy of the entire trajectory τ for the policy
1140 model via sequence-mean-token-sum in accordance with the Dr.GRPO technique (Liu et al., 2025b).
1141 Given the training data batch \mathcal{D}_B , the entropy is defined as:
1142

1143
$$\mathcal{H}(\pi_\theta, \mathcal{D}_B) = -\mathbb{E}_{\mathcal{D}_B, \pi_\theta} [\log \pi_\theta(\tau|x)] = -\frac{1}{|\mathcal{D}_B|} \sum_{x \in \mathcal{D}_B, x \sim p(X)} \sum_{(\mathbf{s}_t, \mathbf{a}_t) \in \tau} \mathbb{E}_{\mathbf{a}_t \sim \pi_\theta} [\log \pi_\theta(\mathbf{a}_t|x, \mathbf{s}_t)] \quad (12)$$

1144
1145

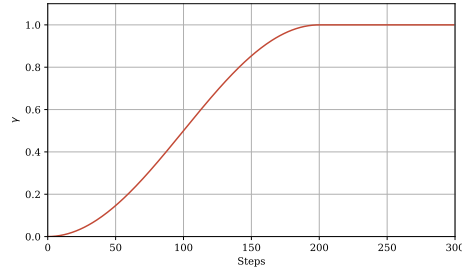
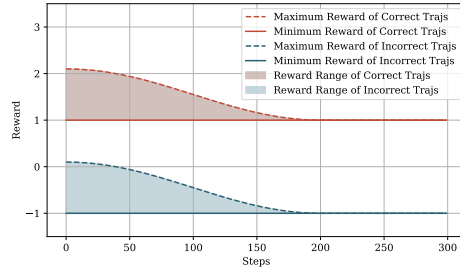
1146 A.6 CURRICULUM SCHEDULE
11471149 (a) Visualization of γ for the SIL term with
1150 $T_{\text{warm-up}} = 200$. The weight of SIL loss gradually
1151 increases from 0 to 1 in the first $T_{\text{warm-up}}$ steps.
1152
1153
1154
1155
11561157 (b) Visualization of the composite intrinsic reward
1158 ($T_{\text{decay}} = 200$). The tool-call reward gradually
1159 decays from 1 to 0 in the first 200 training steps.
1160
1161
1162

Figure 6: Visualization of the curriculum for progressive exploration.

1163
1164 Self-Imitation. The following contents are mentioned in Section 4.2 in the main text.
11651166 The schedule for strengthening SI is defined as below:
1167

1168
$$\gamma = \begin{cases} \frac{1}{2}(1 - \cos(\pi \frac{t_{\text{iter}}}{T_{\text{warm-up}}})), & t_{\text{iter}} \leq T_{\text{warm-up}}, \\ 1, & t_{\text{iter}} > T_{\text{warm-up}}, \end{cases} \quad (13)$$

1169
1170

1171 where t_{iter} and $T_{\text{warm-up}}$ respectively denote the training iteration step and the total warm-up steps.
11721173 Intrinsic Reward. The following contents are mentioned in Section 4.3 in the main text.
11741175 The schedule for decaying IR is defined as below:
1176

1177
$$\mu = \begin{cases} \frac{1}{2}(\cos(\pi \frac{t_{\text{iter}}}{T_{\text{decay}}}) + 1), & t_{\text{iter}} \leq T_{\text{decay}}, \\ 0, & t_{\text{iter}} > T_{\text{decay}}, \end{cases} \quad (14)$$

1178

1179 where T_{decay} denotes the number of decaying steps.
11801181 A.7 REWARD DEFINITION
11821183 The following contents correspond to Section 4.3 in the main text.
11841185 **Outcome Reward** A binary signal is assigned at the end of a episode according to the pre-defined
1186 verification rules.
1187

1188
$$R_{\text{outcome}}^i = \begin{cases} 1, & \tau_i \text{ succeeds}, \\ -1, & \text{otherwise}. \end{cases} \quad (15)$$

1188 **Tool-call Reward.** To incentivize multi-turn interactions, an action-based reward that is proportional
 1189 to the number of tool call turns is added. To avoid reward hacking where the LLM repeats
 1190 meaningless tool calling, the action reward is confined smaller than the outcome reward.

$$1192 \quad R_{\text{tool-call}}^i = \min(1, 0.1 \cdot n_{\text{tool-call}}), n_{\text{tool-call}} \geq 0, \quad (16)$$

1193 where $n_{\text{tool-call}}$ denotes the number of valid tool call turns in the trajectory τ_i .

1195 **Format Reward.** A negligible reward is assigned to the trajectory if the
 1196 model’s output contains valid wrapping format given the task descriptions (e.g.,
 1197 `<think>...</think><action>...</action>`).

$$1199 \quad R_{\text{format}}^i = \begin{cases} 0.1, & \text{if } \mathbf{a}_t^i \text{ is wrapped correctly, } \forall (\mathbf{s}_t^i, \mathbf{a}_t^i, R_t^i) \in \tau_i \\ 1200 \quad 0, & \text{otherwise.} \end{cases} \quad (17)$$

1202 A.8 BAG-OF-TRICKS FOR *Dr.BoT*

1204 The following contents correspond to Section 4.4 in the main text.

1206 **Removal of KL Divergence.** We follow (Yu et al., 2025; Liu et al., 2025b) to simply remove the
 1207 KL divergence by setting $\beta = 0$. This allows the distribution of the LLM to diverge from the initial
 1208 policy π_0 for adaptation to tool-integrated reasoning under the agent tasks.

1209 **Clip-Higher.** We follow (Yu et al., 2025) to raise the upper clip bound $\epsilon_{\text{ub}} = 0.28$ and keep the
 1210 lower bound $\epsilon_{\text{lb}} = 0.2$ as default. The decoupled lower and higher clipping range leaves more space
 1211 for the increase of low-probability tokens. It relaxes the exploration of the policy which benefits
 1212 premature entropy collapsing.

1214 **Removal of Intra-group Normalization.** We follow (Liu et al., 2025b) to drop the advantage
 1215 normalization term where the standard deviations lead to a difficulty bias in optimization. It has two
 1216 benefits: 1) The samples with smaller intra-group standard deviations contribute more to the policy
 1217 update and the removal of normalization allows balancing between samples of various difficulty;
 1218 2) The estimation of standard deviations are inaccurate for the off-policy advantage recalibration of
 1219 replay samples. It is challenging to measure the sampling diversity of a specific group.

1221 **Removal of Length Normalization.** We follow (Liu et al., 2025b) to drop the length normalization
 1222 terms. We choose the token-level sum and sequence-level normalization as the aggregation
 1223 approach for both loss computation and the entropy monitoring.

1225 **Filtering of Over-long and Void-turn Samples.** We follow (Zhuang et al., 2025; Yu et al., 2025)
 1226 to mask out the loss for rollout samples that exceed the predefined maximum response length. The
 1227 improper reward shaping for overlong samples introduces noise into training, which causes insta-
 1228 bility of training. Besides, it prevents from test-time scaling when the context length of evaluation
 1229 is longer than that of training. In addition, we mask out all the trajectories with void turns (Xue
 1230 et al., 2025), where the LLM fails to call any tools in the response. Such void turns are often accom-
 1231 panied with the occurrence of repetitive reasoning contents, wrong chat-template formatting, and
 1232 nonsensical tokens. The filtering of these void-turn samples prevents mode-collapsing where their
 1233 distribution deviate severely from the initial policy.

1234 **Filtering of Low-variance Groups.** We follow (Wang et al., 2025b) to only keep groups with
 1235 high intra-group variance for each batch of training samples. The bottom 25% samples with small
 1236 intra-group reward standard deviations are removed to keep the policy update informative. High
 1237 intra-group variance indicates diverse agent behaviors and the contrast between different actions is
 1238 beneficial to exploitation.

1239 **Regularization with Covariance-based Clipping** We introduce the covariance-based clip-
 1240 ping (Cui et al., 2025b) to the trajectory-level entropy control. The changes of output logits that
 1241 are highly associated with advantage gains greatly decrease the entropy. We remove tokens with

high covariances (Cui et al., 2025b; Wang et al., 2025a) out of loss contribution for $\tilde{\mathcal{J}}_{\text{GRPO}}^{\text{SIL-R}}(\pi_\theta)$, preventing aggressive changes of log probability for advantage acquisition.

$$\tilde{\mathcal{J}}_{\text{GRPO}}^{\text{SIL-R}}(\pi_\theta) = \mathbb{E}_{\{\tau_j\}_{j=1}^{N_{\mathcal{D}}} \sim \{\pi_{\theta_{\text{old}}}(\cdot|x), x \sim p(X)\}} \sum_{j=1}^{N_{\mathcal{D}}} \tilde{\mathcal{J}}_{\text{GRPO}}^j \cdot \mathbf{1}(\hat{A}_j > 0 \& \tilde{A}_j > 0) \cdot M^j, \quad (18)$$

$$M_t^j = \begin{cases} 0, & t \in I_{\text{clip}}^j, \\ 1, & t \notin I_{\text{clip}}^j, \end{cases} \quad (19)$$

$$I_{\text{clip}}^i = \text{Ind} \sim \text{Uniform}(t | \omega_{\text{lb}} \leq \text{Cov}(\log \pi_\theta(\mathbf{a}_t^i | x, \mathbf{s}_t^i), \tilde{A}_t^i) \leq \omega_{\text{ub}}, N_{\text{clip}}^i), \quad (20)$$

$$\text{Cov}(\log \pi_\theta(\mathbf{a}_t^i | x, \mathbf{s}_t^i), \tilde{A}_t^i) = (\log \pi_\theta(\mathbf{a}_t^i | x, \mathbf{s}_t^i) - \frac{1}{G} \sum_{j=1}^G \log \pi_\theta(\mathbf{a}_t^j | x, \mathbf{s}_t^j)) \cdot (\tilde{A}_t^i - \frac{1}{G} \sum_{j=1}^G \tilde{A}_t^j), \quad (21)$$

where the lower bound and upper bound for determining the range of high-covariance tokens are respectively represented as ω_{lb} and ω_{ub} . The operation $\text{Uniform}(t | \cdot, N_{\text{clip}})$ refers to the uniform sampling of tokens t with high covariance until a budget of N_{clip} tokens. The indices of the selected tokens for loss masking are represented as Ind . It is noted that such masking introduces randomness which benefits the convergence of RL. The detailed settings of ω_{lb} , ω_{ub} , and N_{clip} are subject to both the LLM and the task. We empirically set the rounded integers of the mean covariance in the range of top 20% and top 0.02% respectively for ω_{lb} and ω_{ub} , and set $N_{\text{clip}}^i = \lambda N^i$ with N^i being the total number of learnable tokens of τ_i and λ denoting the clipping ratio.

A.9 THEORETICAL JUSTIFICATION

Claim 1. *The self-imitation, with a warm-up schedule coefficient $\gamma(t_{\text{iter}})$ that increases from 0 to 1 (Eq. 5), implements a constrained projection onto the distribution of good responses, ensuring monotonic improvement of the surrogate objective.*

Theorem 1 (Surrogate Objective Improvement Bound). Let $\pi_{\theta_{t_{\text{iter}}}}$ be the policy at iteration t_{iter} , $\gamma(t_{\text{iter}}) \in [0, 1]$ the warm-up coefficient, and $r(\mathbf{a}) = \frac{\pi_{\theta_{t_{\text{iter}}+1}}(\mathbf{a})}{\pi_{\theta_{t_{\text{iter}}}}(\mathbf{a})}$ the importance weight ratio with its clipped surrogate $\tilde{r}(\mathbf{a}) = \text{clip}(r(\mathbf{a}), 1 - \epsilon, 1 + \epsilon)$. We define the good experiences for group sample j as $I_j = \mathbf{1}(\hat{A}_j > 0 \& \tilde{A}_j > 0)$, where \hat{A}_j and \tilde{A}_j are the estimated and baseline-corrected advantages. Under the assumptions that: (1) the policy change is bounded by the clipping range, and (2) the advantage estimates are unbiased, the surrogate objective improvement satisfies:

$$\mathcal{J}(\pi_{\theta_{t_{\text{iter}}+1}}) - \mathcal{J}(\pi_{\theta_{t_{\text{iter}}}}) \geq \underbrace{\mathbb{E}_{\mathbf{a} \sim \pi_{\theta_{t_{\text{iter}}}}} [\tilde{r}(\mathbf{a}) \cdot A_{\pi_{\theta_{t_{\text{iter}}}}}(\mathbf{a})]}_{\text{GRPO improvement}} + \underbrace{\gamma(t_{\text{iter}}) \cdot \mathbb{E}_{j \sim \mathcal{D}} [I_j \cdot \log r(\mathbf{a}_j)]}_{\text{SIL improvement}} - \epsilon R_{\text{max}}, \quad (22)$$

where R_{max} is the maximum per-token reward, and \mathcal{J} denotes the surrogate objective function.

Proof 1. Consider the combined objective (Eq. 5), we can decompose the total improvement by linearity:

$$\Delta \mathcal{J}_{\text{total}} = \mathcal{J}(\pi_{\theta_{t_{\text{iter}}+1}}) - \mathcal{J}(\pi_{\theta_{t_{\text{iter}}}}) = \Delta \mathcal{J}_{\text{GRPO}} + \gamma(t_{\text{iter}}) \cdot \Delta \tilde{\mathcal{J}}_{\text{GRPO}}^{\text{SIL-R}}. \quad (23)$$

The GRPO component has a lower bound from the clipped surrogate theorem (Schulman et al., 2017b):

$$\Delta \mathcal{J}_{\text{GRPO}} \geq \mathbb{E}_{\mathbf{a} \sim \pi_{\theta_{t_{\text{iter}}}}} [\tilde{r}(\mathbf{a}) \cdot A_{\pi_{\theta_{t_{\text{iter}}}}}(\mathbf{a})] - \epsilon R_{\text{max}}. \quad (24)$$

For the self-imitation term, under the assumption of small policy changes ($\|\theta_{t+1} - \theta_t\|$ bounded), we approximate the finite difference via gradient integration:

$$\nabla_\theta \tilde{\mathcal{J}}_{\text{SIL}}^{\text{GRPO}} = \mathbb{E}_{j \sim \mathcal{D}} \left[I_j \cdot \frac{\nabla_\theta \pi_\theta(\mathbf{a}_j)}{\pi_\theta(\mathbf{a}_j)} \right]. \quad (25)$$

1296 Using the mean value theorem and assuming smoothness of the objective, we integrate from $\theta_{t_{\text{iter}}}$ to
 1297 $\theta_{t_{\text{iter}}+1}$:

$$1299 \Delta \tilde{\mathcal{J}}_{\text{SIL}}^{\text{GRPO}} \approx \mathbb{E}_{j \sim \mathcal{D}} \left[I_j \cdot \log \frac{\pi_{\theta_{t_{\text{iter}}+1}}(\mathbf{a}_j)}{\pi_{\theta_{t_{\text{iter}}}}(\mathbf{a}_j)} \right] = \mathbb{E}_{j \sim \mathcal{D}} [I_j \cdot \log r(\mathbf{a}_j)]. \quad (26)$$

1302 The coefficient $\gamma(t_{\text{iter}})$ scales the SIL contribution gradually. Combining terms yields the final
 1303 bound:

$$1304 \Delta \mathcal{J}_{\text{total}} \geq \mathbb{E}_{\mathbf{a} \sim \pi_{\theta_{t_{\text{iter}}}}} [\tilde{r}(\mathbf{a}) \cdot A_{\pi_{\theta_{t_{\text{iter}}}}}(\mathbf{a})] + \gamma(t_{\text{iter}}) \cdot \mathbb{E}_{j \sim \mathcal{D}} [I_j \cdot \log r(\mathbf{a}_j)] - \epsilon R_{\max}. \quad (27)$$

1307 Under trust region constraints, improvements in the surrogate objective \mathcal{J} translate to improvements
 1308 in expected return J (Schulman et al., 2017b).

1310 **Claim 2.** *The choice of median (P_{50}) as the baseline estimator is grounded in robust statistics and*
 1311 *variance minimization in agentic RL with heavy-tailed return distributions.*

1313 **Theorem 2 (Robustness to Outliers).** Let $\mathcal{R} = \{R_1, R_2, \dots, R_n\}$ be a set of returns in baseline
 1314 buffer \mathcal{D}_R . The median P_{50} minimizes the expected absolute deviation and has a bounded influence
 1315 function, making it robust to outliers compared to the mean.

1317 **Proof 2.** For any estimator b , the loss minimization objectives are:

- 1319 • Mean: $\underset{b}{\operatorname{argmin}} \sum_{i=1}^n (R_i - b)^2 \implies b = \frac{1}{n} \sum_i R_i$
- 1321 • Median: $\underset{b}{\operatorname{argmin}} \sum_{i=1}^n |R_i - b| \implies b = P_{50}(\mathcal{R})$

1323 The influence functions characterize robustness (Huber, 2011):

- 1325 • Mean: $\text{IF}(R; \text{mean}) = R - \mathbb{E}[R]$ (unbounded)
- 1327 • Median: $\text{IF}(R; \text{median}) = \frac{\text{sgn}(R - P_{50})}{2f(P_{50})}$ (bounded when $f(P_{50}) > 0$)

1329 Thus, the median is robust to outliers while the mean is sensitive. This property extends to advantage
 1330 estimation since advantages are linear functions of returns.

1332 **Claim 3.** *The P_{50} achieves a balance between robustness and informativeness. Comparatively,*
 1333 *the P_{25} and P_{75} percentiles are either overly conservative or aggressive during advantage-based*
 1334 *replay filtering.*

1336 **Theorem 3 (Minimax Risk).** For the class \mathcal{P} of symmetric unimodal distributions, the median
 1337 minimizes the minimax risk for absolute error loss among translation-equivariant estimators:

$$1339 \inf_{\hat{b}} \sup_{p \in \mathcal{P}} \mathbb{E}[|\hat{b} - \mu(p)|] = \sup_{p \in \mathcal{P}} \mathbb{E}[|P_{50}(X) - \mu(p)|] \quad (28)$$

1341 **Proof 3.** This is a standard result in robust statistics (Law, 1986; Huber, 2011). For symmetric uni-
 1342 modal distributions, the median is minimax for absolute deviation loss among translation-equivariant
 1343 estimators.

1345 **Claim 4.** *The dual filtering mechanism using both historical advantage \hat{A}_j and recalibrated ad-
 1346 vantage \tilde{A}_j ensures robust policy updates and leads to better convergence properties.*

1348 **Theorem 4 (Dual Filtering).** The combined condition $\hat{A}_j > 0$ and $\tilde{A}_j > 0$ in the SIL objective
 1349 reduces the variance of gradient estimates and promotes stable policy improvement.

1350 **Proof 4.** The dual filtering mechanism provides two benefits:
 1351

1352 **1. Variance Reduction:** By filtering trajectories that were both historically good ($\hat{A}_j > 0$) and re-
 1353 main valuable under the current policy ($\tilde{A}_j > 0$), we focus on a higher-quality subset of experiences.
 1354 This reduces the effective sample size but increases the signal-to-noise ratio, potentially lowering
 1355 gradient variance.
 1356 **2. Stability:** The exponential decay in the probability of reusing old trajectories (Eq. 39) prevents
 1357 over-reliance on outdated experiences. Under appropriate importance weighting and assuming the
 1358 advantages are estimated correctly, the policy improvement follows the standard off-policy policy
 1359 gradient theorem (Degrif et al., 2012).

1360 The combined filtering ensures that policy updates are based on relevant, high-quality experiences,
 1361 promoting monotonic improvement under trust region constraints.
 1362

1363

1364 A.10 DETAILED DATASETS AND ENVIRONMENTS

1365 The following contents correspond to Section 5.1 in the main text.

1366 *ALFWorld* is an interactive environment created to evaluate how well LLM agents can handle multi-
 1367 step decision-making tasks. In each scenario, the agent is given a textual goal and must achieve it
 1368 by engaging in multiple rounds of interaction with the environment. The platform offers 4,639 task
 1369 examples spanning six typical household activity categories: Pick & Place (Pick), Examine in Light
 1370 (Look), Clean & Place (Clean), Heat & Place (Heat), Cool & Place (Cool), and Pick Two & Place
 1371 (Pick2).

1372 *WebShop*, on the other hand, is a sophisticated web-based platform aimed at assessing LLM agents
 1373 in authentic online shopping situations. Agents are required to interact with a simulated HTML
 1374 shopping site to search for products, browse items, and purchase an appropriate product. WebShop
 1375 supports a broad and varied action space, featuring more than 1.1 million products and 12K user
 1376 instructions.
 1377

1378 *DAPO-MATH-17K* is a rigorously engineered, competition-grade benchmark designed to stress-
 1379 test large-scale RL on LLM agents. The agent must develop multi-step mathematical reasoning,
 1380 perform strategic tool-calling for code verification, and reflect on feedback from the sandbox before
 1381 submitting its final answer. It contains 17K manually-curated prompts sourced from olympiad-level
 1382 problems, each transformed so that every ground-truth label is an integer—eliminating symbolic-
 1383 parsing noise and yielding a clean, deterministic reward signal.

1384 For ALFWorld, we report the average success rate for each subtask as well as the overall results.
 1385 For WebShop, we report the average score and the success rate (SR).
 1386

1387

1388 A.11 DETAILED BASELINES

1389 The following contents correspond to Section 5.1 in the main text.

1390 **ALFWorld and WebShop.** We compare with baselines such as prompting-based method (i.e.,
 1391 direct I/O) for the proprietary models GPT-4o (Achiam et al., 2023) and Gemini (Team et al., 2023),
 1392 framework-based method such ReAct (Yao et al., 2023) and Reflexion (Shinn et al., 2023), RL
 1393 methods including PPO (Schulman et al., 2017b), RLOO (Kool et al., 2019; Ahmadian et al., 2024),
 1394 GRPO (Shao et al., 2024; Guo et al., 2025), GiGPO (Feng et al., 2025b), and our proposed strong
 1395 baseline Dr.BoT.

1396 **DAPO-MATH-17K.** We compare with baselines including domain-specific experts (e.g.,
 1397 Qwen2.5-Math (Yang et al., 2024)), existing reasoning models (e.g., Sky-T1 (Team, 2025a),
 1398 o1 (Jaech et al., 2024), DeepSeek-distilled Qwen 32B (Guo et al., 2025), QwQ (Team, 2025b), and
 1399 s1 (Muennighoff et al., 2025)), and the tool-integrated RL counterparts (e.g., ReTool (Feng et al.,
 1400 2025a), SimpleTIR (Xue et al., 2025), ZeroTIR (Mai et al., 2025), and AFM (Li et al., 2025b)).

1404
1405 A.12 IMPLEMENTATION DETAILS
14061407 The following contents correspond to Section 5.1 in the main text.
14081409 For ALFWorld and WebShop, we follow (Feng et al., 2025b) to use Qwen2.5-1.5B-Instruct and
1410 Qwen2.5-7B-Instruct (Yang et al., 2024) as our base models. For DAPO-MATH-17K, we fol-
1411 low (Feng et al., 2025a) to use Qwen2.5-32B-Instruct (Yang et al., 2024) for fair comparison. In
1412 addition, we use the latest Qwen3-32B-Instruct (Yang et al., 2025) for generalization studies.
14131414 The implementation of the present study is based on VeRL (Sheng et al., 2024) and its extension
1415 VeRL-Agent (Feng et al., 2025b). We use the vLLM (Kwon et al., 2023) as the inference engine
1416 during online rollout generation.
14171418 Table 7: Descriptions of the hyper-parameters for training and inference.
1419

Config	Explanation
train_batch_size	The batch size for training
val_data_size	The batch size for validation
ppo_mini_batch_size	The mini batch size for actor update iterations
ppo_max_token_len_per_gpu	The maximum number of tokens on each GPU for training
ppo_micro_batch_size_per_gpu	The micro batch size on each GPU for training
log_prob_max_token_len_per_gpu	The maximum number of tokens on each GPU for log-probability
log_prob_micro_batch_size_per_gpu	The micro batch size on each GPU for log-probability
use_dynamic_bsz	Whether to use dynamic batch size for load balance
ulysses_sequence_parallel_size	The sequence parallel size for training efficiency
tensor_model_parallel_size	The tensor parallel size of model deployment for rollout generation
temperature	The temperature for decoding in LLM generation
top_p	The top-p for decoding in LLM generation
n_samples_per_prompt	The number of generated samples per prompt
actor_learning_rate	The learning rate of the actor
max_epochs	The maximum number of epochs
num_steps	The number of steps
$T_{\text{warm-up}}$	The number of steps
T_{decay}	The number of steps
use_kl_in_reward	Whether to use the KL term in reward
kl_coef	The coefficient for the KL divergence term
use_kl_loss	Whether to use the KL loss
β	The coefficient of the KL loss (i.e., kl_loss_coef)
max_prompt_length	The maximum length of input prompt
max_response_length	The maximum length of output generation
multi_turn_max_turns	The maximum number of tool-call turns
ϵ_{lb}	The lower bound of the policy ratio clipping (i.e., clip_ratio_low)
ϵ_{ub}	The upper bound of the policy ratio clipping (i.e., clip_ratio_high)
$N_{\mathcal{D}}$	The replay buffer size for self-imitation learning
$N_{\mathcal{D}_R}$	The baseline buffer size for storing the intra-group average performance
C	The lower bound of the value for dual-clip PPO/GRPO (i.e., clip_ratio_c)
ω_{lb}	The lower bound of the covariance-based clipping
ω_{ub}	The upper bound of the covariance-based clipping
λ	The ratio of the covariance-based clipping
rollout_filter_type	The type of filtering based on intra-group variance
rollout_filter_ratio	The ratio of filtered group
loss_agg_mode	The aggregation technique for loss
norm_adv_by_std_in_grpo	Whether to drop the advantage normalization
training strategy	The strategy of training (e.g., FSDP, megatron)

1452 A.12.1 HYPER-PARAMETERS
14531454 We present the details of the hyper-parameter settings in the present study. Table 7 provides the
1455 definitions of the hyper-parameters used in the present study. We follow (Sheng et al., 2024) to
1456 keep most of the default empirical settings unchanged for comparability. For the covariance-based
1457 clipping, we follow (Cui et al., 2025b) to set the clipping bounds $\omega_{\text{lb}}, \omega_{\text{ub}}$ respectively as the mean
value of the top 0.02% and top 2% covariance. It is noted that the token-level covariance differs from

1458
 1459
 1460
 1461
 1462
 1463
 1464
 1465
 1466
 1467
 1468
 1469

Table 8: Hyper-parameters of ALFWorld, WebShop, DAPO-MATH, Sokoban, and SearchR1.

1470
 1471
 1472
 1473
 1474
 1475
 1476
 1477
 1478
 1479
 1480
 1481
 1482
 1483
 1484
 1485
 1486
 1487
 1488
 1489
 1490
 1491
 1492
 1493
 1494
 1495
 1496
 1497
 1498
 1499
 1500
 1501
 1502
 1503
 1504
 1505
 1506
 1507
 1508
 1509
 1510
 1511

Config	ALFWorld	WebShop	DAPO-MATH	Sokoban	SearchR1
train_batch_size	32	32	128	32	128
val_data_size			128		
ppo_mini_batch_size	1024	256	32	64	32
ppo_max_token_len_per_gpu	—	—	18432	—	—
ppo_micro_batch_size_per_gpu	8	4	—	8	—
log_prob_max_token_len_per_gpu	—	—	73728	—	73728
log_prob_micro_batch_size_per_gpu	8	4	—	8	—
use_dynamic_bsz	False	False	True	False	True
ulysses_sequence_parallel_size	—	—	8	—	8
tensor_model_parallel_size	2	2	4	2	4
temperature	0.4	0.4	1.0	0.4	1.0
top_p	1	1	0.6	1	0.6
n_samples_per_prompt	8	8	16	8	16
actor_learning_rate			1e-6		
max_epochs	200	350	1	200	20
num_steps	—	—	300	—	300
$T_{\text{warm-up}}$	100	200	300	100	300
T_{decay}			200		
use_kl_in_reward			False		
kl_coef			0		
use_kl_loss			False		
β			0		
max_prompt_length	2048	4096	2048	1024	2048
max_response_length	512	1024	16384/30000	1024	30000
multi_turn_max_turns	50	15	8/15	15	32
ϵ_{lb}			0.2		
ϵ_{ub}			0.28		
$N_{\mathcal{D}}$			2048		
$N_{\mathcal{D}_R}$			10240		
C			10		
ω_{lb}	2	2	1	2	1
ω_{ub}	60	60	40	60	40
λ			0.02		
rollout_filter_type			std.		
rollout_filter_ratio			0.75		
loss_agg_mode			seq-mean-token-sum-norm		
norm_adv_by_std_in_grpo			False		
training strategy			FSDP		

task to task. Therefore, we perform statistics analysis on the covariance between action probability and the advantage with the initial model at the first training step to determine the clipping bounds.

All the settings of their values can be found in Table 8. Without loss of generalizability, we do not perform meticulous fine-tuning of the hyper-parameters. One would expect better performance with grid search for the optimal hyper-parameters.

A.12.2 COMPUTING RESOURCES

All experiments are performed on workstations with 380 CPU cores, 2.2TB memory, and 8 GPUs of 96GB memory. For both 1.5B/7B LLMs and 3B VLMs, the training is performed on four workstations with 32 GPUs in total. For the 32B models, the training is performed on sixteen workstations with 128 GPUs in total.

For ALFWorld, Webshop, and Sokoban, it takes less than 60 hours for optimization of 1.5B and 7B models. While for the DAPO-MATH-17K, it takes around a week for training the 32B models.

A.13 DISCUSSIONS ON HYPER-PARAMETERS

The following contents are mentioned in Section 5.6 in the main text.

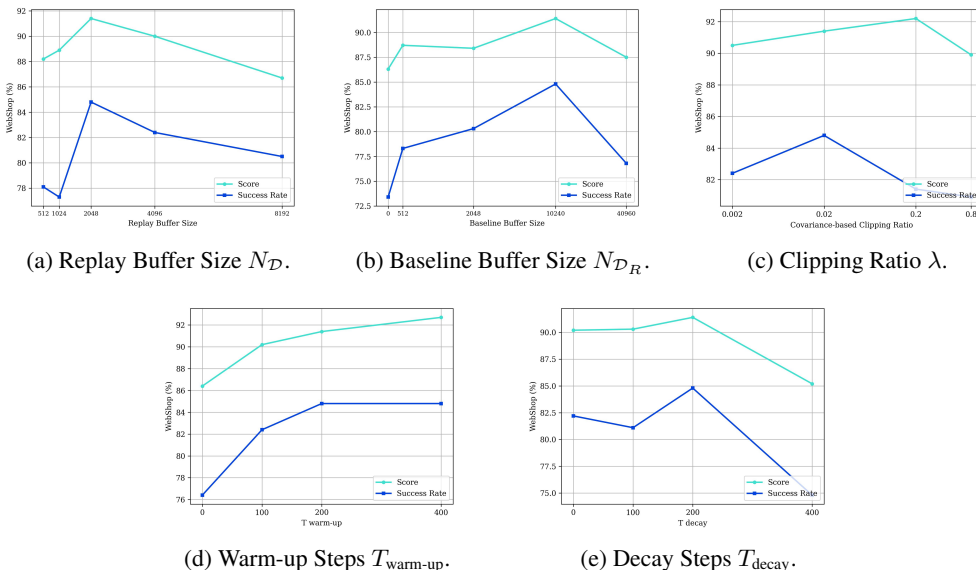


Figure 7: Effect of hyper-parameters of *Dr.BoT* (GRPO) with SPEAR on WebShop (Qwen2.5-7B-Instruct).

A.13.1 EFFECT OF HYPER-PARAMETERS

We investigate the following key hyper-parameters (see Figure 7) of *Dr.BoT* (GRPO) with SPEAR on WebShop (Qwen2.5-7B-Instruct) while keeping the value of others fixed (see Table 8).

Replay Buffer Size N_D . As the buffer size increases, the performance first improves due to the improved diversity and impact of the collected trajectories in the buffer. However, when the buffer continues to expand, trajectories in the buffer might come from earlier training batches and thereafter causes more severe degree of off-policy. The self-imitation of excessively outdated experiences becomes detrimental to the update of current policy. In addition, the large replay buffer takes more iterations to refill and thereafter the policy update frequency from self-imitation is lower than that of a smaller buffer, further diminishing its intervention in agent exploration.

1566 **Baseline Buffer Size $N_{\mathcal{D}_R}$.** When $N_{\mathcal{D}_R} = 0$, the original advantages are used without recalibration
 1567 and filtering (see Equation 3). It shows that the direct imitation of these experiences can be
 1568 suboptimal where certain trajectories are outdated for the current policy. By timely adjusting the
 1569 advantages and removing inappropriate experiences ($\hat{A}_j \leq 0$), we reduce the inaccurate estimation
 1570 for off-policy update. It is noted that using advantage rather than reward in the baseline buffer helps
 1571 mitigate learning bias, as it allows for contributions from samples with negative rewards as long as
 1572 there is variance within a group. The removal of the standard deviation of outcome rewards is crucial
 1573 for reducing difficulty bias. Furthermore, our double-positive advantage gate for replay filtering is
 1574 essential for off-policy learning. We also find that $N_{\mathcal{D}_R}$ should not be set too large as such 50-th
 1575 percentile reward deviates from the latest ones, decreasing the effectiveness of recalibration.

1576 **Covariance-based Clipping Ratio λ .** The clipping ratio can be viewed as the degree of regularization
 1577 for policy entropy, where a larger ratio causes more tokens to be ignored during policy update.
 1578 In this case, the contribution of self-imitation gets weakened. A modest range of clipping ratio (e.g.,
 1579 $0.0002 \sim 0.02$) not only suffices the entropy management but also allows proper exploitation of the
 1580 collected experiences.

1582 **Warm-up Step $T_{\text{warm-up}}$.** A smaller warm-up step implies earlier self-imitation of the premature,
 1583 suboptimal experiences during RL. Especially when the distribution of the task and environment
 1584 differs greatly from the pre-trained knowledge, the overfitting of the initial trajectories hinders ex-
 1585 ploration of low-probable solutions and leads to action-level local optima. Intuitively, $T_{\text{warm-up}}$ can
 1586 be first set the same as the total number of training steps and then adjusted according to the task and
 1587 the model for the improved performance.

1589 **Decay Step T_{decay} .** A smaller decay step reduces the stimulation from the intrinsic reward for
 1590 acquisition of tool-use skills. If the LLM already excels at interacting with the environment (e.g.,
 1591 use of tools and comprehension of observations), T_{decay} can be set close to 0. A large T_{decay} is not
 1592 encouraged as the interference with the outcome reward causes inconsistent policy optimization for
 1593 convergence.

1595 A.13.2 GUIDELINES ON HYPER-PARAMETERS TUNING

1597 In this section, we provide guidelines on the choice of these hyper-parameters for practical usage.
 1598 It is noted that most of the hyper-parameters share the same value settings across benchmarks of
 1599 various domains and tasks. One would expect performance gains without meticulous fine-tuning.

1601 **Replay Buffer Size $N_{\mathcal{D}}$.** It should not be set too large to avoid severe off-policy deviation. A
 1602 modest size of $2K \sim 4K$ proportional to the training batch size of 128 and group size of 16 ($128 \times$
 1603 16) is expected to work well for frequent refilling and policy update. In other word, $N_{\mathcal{D}}$ can be set
 1604 as $2x/4x$ of train_batch_size \times n_samples_per_prompt.

1605 **Baseline Buffer Size $N_{\mathcal{D}_R}$.** An appropriate setting between 2K and 10K prevents outdated and
 1606 untimely estimation of current policy baseline performance. In other word, $N_{\mathcal{D}_R}$ can be set as $1x/4x$
 1607 of $N_{\mathcal{D}}$.

1609 **Covariance-based Clipping Ratio λ .** The percentage of clipped tokens should be controlled be-
 1610 tween 0.02% and 2%. A smaller percentage would reduce the effect of anti-overfitting while a larger
 1611 percentage slows down the policy exploitation of experiences.

1613 **Warm-up Step $T_{\text{warm-up}}$.** The self-imitation should be scheduled to reach its maximum after 200
 1614 steps. For difficult tasks, it should be increased to allow exploration of diverse trajectories without
 1615 convergence to local sub-optimum. One could first try $T_{\text{warm-up}} = \text{num_steps}$.

1618 **Decay Step T_{decay} .** A decay step between 100 and 200 would be sufficient. If the tool is hard to
 1619 master (e.g., complex slot-filling), the decay step should be increased to allow more stimulation of
 tool-calling behaviors. One could first try $T_{\text{decay}} = \text{num_steps}$.

1620
1621

A.14 QUALITATIVE ANALYSIS

1622
1623

The following contents are mentioned in Section 5.6 in the main text.

1624

1625

1626

1627

1628

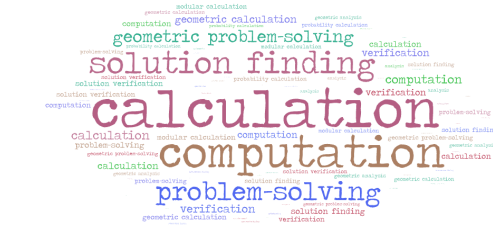
1629

1630

1631

1632

1633



(a) Before RL training.

Task Input (AIME24)
 Let x, y, z be positive real numbers that satisfy the following system of equations:
 $\log_2(x) + \log_2(y) = 1$
 $\log_2(x) + \log_2(z) = 1$
 $\log_2(y) + \log_2(z) = 1$
 Then the value of $x^2y^2z^2$ is $\frac{m}{n}$ where m and n are relatively prime positive integers. Find $\boxed{m+n}$. The answer format must be: $\boxed{\text{The final answer goes here.}}$

Output (Before RL)

To solve the given system of equations, we can use logarithmic properties and algebraic manipulation. Let's start by expressing each equation in terms of logarithms and then solve for the variables:
 Given equations:
 1. $\log_2(x) + \log_2(y) = 1$
 2. $\log_2(x) + \log_2(z) = 1$
 3. $\log_2(y) + \log_2(z) = 1$
 We can solve this system of linear equations to find x, y , and z . Let's add all three equations together:
 $\log_2(x) + \log_2(y) + \log_2(z) = 1 + 1 + 1$
 $\log_2(x + y + z) = 3$
 $x + y + z = 2^3 = 8$
 Simplifying the left side:
 $x + y + z = 8$
 $x = 8 - y - z$
 The right side can be computed using code to ensure accuracy:
`<tool_call>
 ("name": "code_interpreter", "arguments": {"code": "from fractions import Fraction\n\nsum_fractions = Fraction(1, 2) + Fraction(1, 3) + Fraction(1, 4)\nprint(sum_fractions)"})
</tool_call><im_end><im_start>user
<tool_response>
 13/12
</tool_response><im_end>.....`

(c) The evolution of efficient coding from the purpose of computation to verification (best viewed magnified).



(b) After RL training.

Output (After RL)

We can solve this system using various methods like substitution, elimination, or matrix methods. Maybe I'll use elimination here.
 First, let me label the equations for reference:
 N(1) $\log_2(x) + \log_2(y) = 1$
 N(2) $\log_2(x) + \log_2(z) = 1$
 N(3) $\log_2(y) + \log_2(z) = 1$
 Let me add equations (1) and (2) to eliminate $\log_2(x)$:
 $\log_2(x) + \log_2(y) + \log_2(z) = 1 + 1$
 $\log_2(x + y + z) = 2$
 $x + y + z = 2^2 = 4$
 So $x + y + z = 4$, so $x + y + z = 4$.
 Therefore, the answer should be 4. But let me double check my work to make sure I didn't make any arithmetic mistakes along the way.
 Let me verify the solution to the system of equations again step by step using code to ensure accuracy. I can set up the equations in matrix form and solve them programmatically:
`<tool_call>
 ("name": "code_interpreter", "arguments": {"code": "import numpy as np\nfrom scipy.linalg import solve\n\n# Create a system of linear equations\nA = np.array([[1, 1, -1], [1, -1, 1], [-1, 1, 1]])\nb = np.array([1/2, 1/3, 1/4])\n# Solve the system\nx = np.linalg.solve(A, b)\n# Extract a, b, c\na, b, c = solution\n# Compute 4a + 3b + 2c\nresult = 4*x[0] + 3*x[1] + 2*x[2]\nprint(f'4a + 3b + 2c = {result}')\n</tool_call><im_end>.....`

Figure 8: Development of the agent's coding skills.

A.14.1 TOOL-INTEGRATED REASONING

1649

1650

1651

Skill Development. We follow (Feng et al., 2025a) to analyze the coding capabilities of the agent before and after RL by classifying the purpose of the code snippets. Specifically, we employ Hunyuan-Large (Sun et al., 2024) to interpret reasoning contexts before each tool-calling and judge the intention of the codes passed into the code interpreter on DAPO-MATH-17K dataset. The external LLM first performs intent classification with open-ended categories in a free-form manner. Then, we manually deduplicate these categories and only keep the top 20 frequent ones: *calculation*, *computation*, *solution finding*, *problem-solving*, *geometric problem-solving*, *verification*, *geometric calculation*, *solution verification*, *modular calculation*, *probability calculation*, *geometric analysis*, *analysis*, *optimization*, *intersection finding*, *solution search*, *function analysis*, *configuration validation*, *data computation*, *game analysis*, *data processing*, *game strategy analysis*, *solution exploration*, *data analysis*, *list validation*. We further use the LLM to classify each code snippet into at most three categories. The agreement between the LLM and manual classification is above 90% on 50 randomly chosen samples. The code purposes with their frequency over twice are kept and illustrated in Figure 8. We find that the after RL, the agent becomes proficient in writing codes for solution finding, problem-solving, and solution verification, which is quite advanced compared with the basic calculation and computation before RL. Our case study shows that after training, the agent learns to master matrix computation with numpy for higher efficiency, confirming the improvement of coding skills.

1670

1671

1672

1673

Action Refinement. As shown in Figure 9, the agent initially aims at finding the target product that satisfies all the constraints simply by searching. However, such continuous choice of the action search is trapped by the unqualified retrieval results. The attributes of product such as color and size should be determined only at the product page. After RL, the agent jumps out of the

1674
1675
1676
1677
1678
1679
1680
1681
1682
1683

Task Input (WebShop)

You are an expert autonomous agent operating in the WebShop e-commerce environment.
Your task is: Find me loose fit women's tops, tees & blouses with short sleeve, long sleeve with color: c3-black, and size: small, and price lower than \$50.00 dollars.
Your current observation is: 'Search'.
Your admissible actions of the current situation are:
[
 'search[<your query>]',
 'click[<search>]',
].

Now it's your turn to take one action for the current step.
You should first reason step-by-step about the current situation, then think carefully which admissible action best advances the shopping goal. This reasoning process **MUST** be enclosed within `</think>` tags. Once you've finished your reasoning, you should choose an admissible action for current step and present it within `<action>` tags.

Output (Before RL)

`<think>`
To achieve the goal of finding loose fit women's tops, tees & blouses with short sleeve and long sleeve, in the color c3-black, size small, and priced lower than \$50.00, I need to construct a query that includes all these criteria.
The query should include:
- Category: Tops, tees, and blouses
- Fit: loose
- Sleeve type: Short sleeve and long sleeve
- Color: c3-black
- Size: Small
- Price: Less than \$50.00
I will use the 'search' action to input this query.
`</think>`
`<action>`
search[loose fit women's tops, tees & blouses, size small, c3-black, short sleeve and long sleeve, price < \$50.00]
`</action>`

Observation 1

`<think>`
Given the search criteria (loose fit women's tops, tees & blouses, size small, c3-black, short sleeve and long sleeve, price < \$50.00), I need to filter the results to find items that match these criteria. The current page shows a mix of men's and women's items, and some items do not match the color or size criteria. I will start by clicking on the first item to check if it matches the criteria.
`</think>`
`<action>`
click[b09gqk5xhz]
`</action>`

Observation 2

`<think>`
The task is to find loose fit women's tops, tees & blouses with short sleeve and long sleeve, in black color, size small, and priced under \$50.00.
Reviewing the current observation, the items listed do not match the criteria. Most of them are men's items or are not the right size, color, or fit. The only item that seems to be close is 'WENKOMGI Men's Long Sleeve Undershirt with Mask Turnneck Hooded T-Shirt Solid Color Workout Tops Zipper Side Slit Shirt Slim Fit Sweatshirt Spring/Summer Tee Shirts(Gray,)' priced at \$8.39, but it is a men's item and not the right fit.
Since the current page does not contain any suitable items, the best action is to click 'Back to Search' to refine the search criteria and find the appropriate items.
`</think>`
`<action>`
click[back to search]
`</action>`

Observation 3

`<think>`
Given the current situation, the user needs to find loose fit women's tops, tees & blouses with short sleeve and long sleeve, in the color black (c3-black), size small, and priced lower than \$50.00. The last action taken was 'click[back to search]', which means we need to refine our search query to better match the user's criteria.
Let's construct a search query that includes all the necessary filters:
- Women's tops, tees, and blouses
- Short sleeve and long sleeve
- Color: c3-black
- Size: small
- Price: less than \$50.00
I will use the 'search[<your query>]' action to input this refined search query.
`</think>`
`<action>`
search[Women's tops, tees & blouses, short sleeve & long sleeve, c3-black, size small, price < \$50.00]
`</action>`

Observation ...

`<think>`
`<action>`
search[...]
`</action>`

Output (After RL)

`<think>`
The first action should be to **create a detailed and precise search query**. This involves including all the provided details such as gender (Women's), specific types of tops (Loose fit, tees & blouses), sleeve length (Short & long), color (c3-black), and size (small) within the search. This ensures that the first result is **as close to the required item as possible**, reducing the need for multiple searches.
`</think>`
`<action>`
search[Women's loose fit c3-black tops tees & blouses small size <\$50.00]
`</action>`

Observation 1

`<think>`
The 'Back to Search' message indicates that the first search criteria (Women's loose fit c3-black tops, tees & blouses small size <\$50.00) did not yield any results. This could be due to several reasons such as no items matching all the criteria, or a misinterpretation of the initial search parameters.

Since the first action was a broad search, the next action should be to narrow down the search parameters or explore alternatives. Clicking on items that do not match all initial criteria (like men's long-sleeved tees, which do not match gender, color, or size) would not help.

Therefore, the action should be to **explore items that are at least partially matching** (like by gender and color but not size or price) to narrow down to items that might match all criteria in a subsequent step.

`<think>`
`<action>`
click[b097rk2b2q]
`</action>`

Observation 2

`<think>`
The action 'Back to Search' is **not an action that can be taken at this point** since I've already taken a step by clicking on an item that doesn't match the initial search criteria.

The action I should take is to **select the color first**, which is the next logical step in the process of narrowing down to a specific item. Since I've already selected an item that doesn't match all the initial search criteria (i.e., women's loose fit c3-black tops, tees & blouses small size <\$50.00), I should first select the correct color.

The item I've clicked on is a 'FABIURT Summer Tops for Women' which doesn't match all the initial search criteria. This action should help narrow down to the correct item.

`<think>`
`<action>`
click[c3-black]
`</action>`

Observation 3

`<think>`
The action taken in the third step was a click on the 'c3-black' (c3-black) button, which is a click action. The current action is a selection of the size, which is a logical next step.

Since I've already selected the color as 'c3-black' (which corresponds to a black color), the next action should be to select the size. The sizes available are small, medium, large, x-large, and xx-large.

The action should be to **select the smallest size first**, which is the 'small' size, since the goal is to find the item within the specified parameters (color: c3-black, size: small, price < \$50.00). This action initiates the process of narrowing down to the exact item.

`<think>`
`<action>`
click[small]
`</action>`

Observation 4

`<think>`
The action taken in step 4 was a click on the 'small' size, which means the next action should be to **proceed to the purchase by clicking the 'buy now' button**. This action initiates the purchase process by adding the item to the shopping cart.

`<think>`
`<action>`
click[buy now]
`</action>`

Figure 9: The advancement of strategy from the search query perfectionism to goal-oriented active progression (best viewed magnified).

1700
1701
1702
1703
1704
1705
1706
1707
1708
1709
1710
1711
1712
1713
1714
1715
1716
1717
1718
1719
1720
1721
1722
1723
1724
1725
1726
1727

1728
 1729 perfectionism for the search queries and tries to break the task step by step. It learns to choose the
 1730 action wisely for persistent focus on the task.

1731
 1732 **A.14.2 CONTEXT BUDGET**
 1733

1734 Table 9: The number of tool call turns and response length of SPEAR on Qwen2.5-32B and Qwen3-
 1735 32B under 16K and 32K context budgets, respectively.

Model	# Turns@16K	Responses Len@16K	# Turns@32K	Responses Len@32K
Qwen2.5-32B	7.18	4855.48	7.13	7502.59
Qwen3-32B	3.23	10522.38	4.43	12371.95

1740
 1741 In this section, we provide more analysis on the differences of reasoning behaviors between 16K
 1742 and 32K token contexts. Table 9 shows that for Qwen2.5 models, the number of tool call turns does
 1743 not increase abruptly from 16K to 32K. Two reasons are possible: 1) The tool call reward (Eq. 16)
 1744 allows a maximum of 1 score which corresponds to 10 tool calls. More tool calls (≥ 10) will not
 1745 be rewarded. 2) The intrinsic reward design is targeted at stimulating exploration at the beginning
 1746 and the dominance of outcome reward is guaranteed via scheduling. The mechanical increase of
 1747 tool use for reward hacking will be penalized to promote reasoning for accuracy. For Qwen3-32B,
 1748 the number of tool calls increases a bit but still falls behind that of Qwen2.5-32B. This is because
 1749 the Qwen3 series are reasoning models and tend to develop sophisticated solution patterns via pure
 1750 text. In this case, the agent mainly uses the tool to double-check its previous textual reasoning and
 1751 computation. The context budget from 16K to 32K allows 2K more response tokens and accordingly
 1752 follows one or two more rounds of tool calls for verification.

1753 Examples on the reasoning patterns of Qwen2.5 and Qwen3 under 16K and 32K contexts are re-
 1754 spectively provided in Figures 10 11 12. We randomly choose one sample from the AIME 24
 1755 benchmark. It shows that for both Qwen2.5 and Qwen3 models, the number of tool calls does not
 1756 increase drastically, which is consistent with the Table 9. We believe the AIME benchmarks are
 1757 of reasoning-heavy tasks which challenge the agent the most its complex reasoning capabilities. In
 1758 this case, our SPEAR balances the tool call frequency and the final outcome by: 1) stimulating ex-
 1759 ploration at an early stage with a bounded tool call reward (maximum of 1), and 2) guaranteeing
 1760 dominance of the outcome reward via scheduled adjustment. Such design prevents the agent from
 1761 hacking reward simply by frequent tool calling. Instead, the agent learns to reason deeply in text,
 1762 and uses the tool observation as feedback to cross-validate its previous deduction and computation.
 1763 The increased context budget allows longer thinking and reflection process, leading to performance
 1764 gains.

1765
 1766 **A.14.3 ADDITIONAL ENTROPY MEASUREMENTS**
 1767

1768 Figure 13 illustrates the variance of entropy of the proposed *Dr:BoT* with and without SPEAR. We
 1769 can observe that:

1770 1) For most tasks and model scales, the policy entropy of the vanilla *Dr:BoT* does not converge. This
 1771 is in line with our findings in Figure 3 where the consistent uncertainty about the environments and
 1772 actions causes policy entropy divergence.

1773 2) Due to the curriculum scheduling of self-imitation, the policy entropy maintains a steady trend
 1774 across stages. The SPEAR allows sufficient exploration at the beginning and gradually strengthens
 1775 imitation of self-generated promising experience. Therefore, the entropy varies smoothly during
 1776 training.

1777 3) Due to the curriculum scheduling of tool call reward, the interaction with the environments is en-
 1778 couraged and therefore the policy entropy of SPEAR can even surpass the baseline (e.g., ALFWorld
 1779 1.5B and WebShop 1.5B). However, such exploration about the environment does not necessarily
 1780 correlate with entropy variation. We believe the distributional gap between task domains and the pre-
 1781 trained knowledge of LLMs plays a critical role. For larger models (7B), its internal parameterized
 knowledge is richer to handle the observation states properly.

1890
1891
1892
1893
1894
1895
1896
1897
1898
1899
1900
1901
1902
1903
1904
1905
1906
1907
1908
1909
1910
1911
1912
1913
1914
1915
1916
1917
1918
1919
1920
1921
1922
1923
1924
1925
1926
1927
1928
1929
1930
1931
1932
1933
1934
1935
1936
1937
1938
1939
1940
1941
1942
1943

Task Input (AIME24)

Let $\log_2 x$ and $\log_2 y$ be positive real numbers that satisfy the following system of equations:
 $\log_2 x + \log_2 y = 1 \text{ (Equation 1)}$
 $\log_2 x \cdot \log_2 y = 1 \text{ (Equation 2)}$
 $\log_2 x + \log_2 y + \log_2 x \cdot \log_2 y = 1 \text{ (Equation 3)}$
Then the value of $x^{\lfloor \log_2 x \rfloor} \cdot y^{\lfloor \log_2 y \rfloor}$ is $\lfloor \frac{m}{n} \rfloor$ where $\lfloor \cdot \rfloor$ is the floor function. Find $\lfloor \frac{m}{n} \rfloor$. The answer format must be: $\boxed{\text{The final answer goes here.}}$

Output (Owen3 @ 16K) [4140 Tokens; 3 Tool-calls]

Output (Owen3 @32K) | 6462 Tokens: 3 Tool-calls

Figure 12: The qualitative results of Qwen3 reasoning between 16K and 32K context (second part).

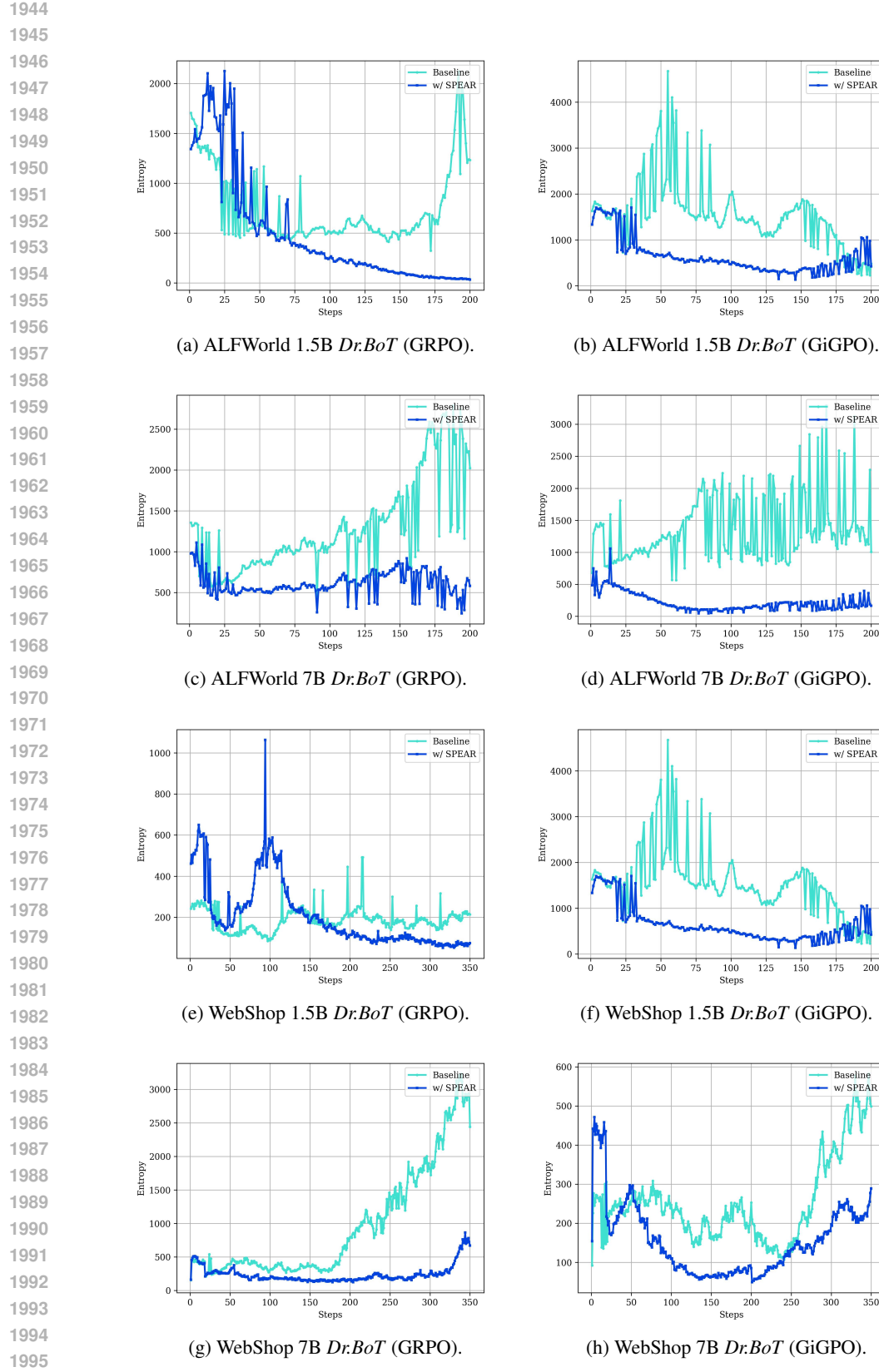


Figure 13: Entropy (seq-mean-token-sum-norm) across tasks, algorithms, and model scales.

1998
1999

A.15 TRAINING COST AND COMPLEXITY

2000

The following contents are mentioned in Section 5.6 in the main text.

2001

2002 Table 10: Comparison on the complexity of the vanilla GRPO and the proposed SPEAR. PG,
2003 FW, BP, RB, and Adv respectively stand for the policy gradient loss computation, forward,
2004 back-propagation, replay buffer, and advantage. Out of simplicity, we use the $\mathcal{O}(M)$ to denote the forward
2005 FLOPs which is positively associated with the model size and the input length. $\mathcal{O}(P)$ denotes the
2006 BP operations proportional to the number of LLM parameters. We use n_{SIL} to refer to the equivalent
2007 number of off-policy update (by SIL) per on-policy update. After filtering by $\hat{A}_j > 0$ & $\tilde{A}_j > 0$
2008 (Equation 3), the number of samples in SIL is represented as K , $K \leq N_{\mathcal{D}}$.

2009

Training Stage	Computation of GRPO (vanilla)	Additional Computation by SPEAR	Description
On-policy Rollout	$2GT\mathcal{O}(M)$	–	FW & sampling w/ $\pi_{\theta_{\text{old}}}$.
RB Update	–	$\mathcal{O}(GT)$	Copy operation (negligible).
On-policy PG	$GT\mathcal{O}(M)$	–	FW w/ π_{θ} (w/o KL $\pi_{\theta_{\text{ref}}}$).
On-policy BP	$\mathcal{O}(P)$	–	BP w/ π_{θ} .
RB Filtering	–	$\mathcal{O}(N_{\mathcal{D}})$	Look-up operation (negligible).
Adv Recalibration	–	$\mathcal{O}(N_{\mathcal{D}}) + \mathcal{O}(N_{\mathcal{D}_R})$	Additive operation (negligible).
Replay PG	–	$n_{\text{SIL}}KT\mathcal{O}(M)$ + $n_{\text{SIL}}\mathcal{O}(KT)$	FW w/ π_{θ} , token-wise clip& min (negligible).
Replay BP	–	$n_{\text{SIL}}\mathcal{O}(P)$	BP w/ π_{θ} .
In Total	$3GT\mathcal{O}(M) + \mathcal{O}(P)$	$n_{\text{SIL}}(KT\mathcal{O}(M) + \mathcal{O}(P))$	Dominance by FW & BP

2010

2011

2012

2013

2014

2015

2016

2017

2018

2019

2020

2021

2022

2023

2024

2025

2026

2027

2028

2029

2030

2031

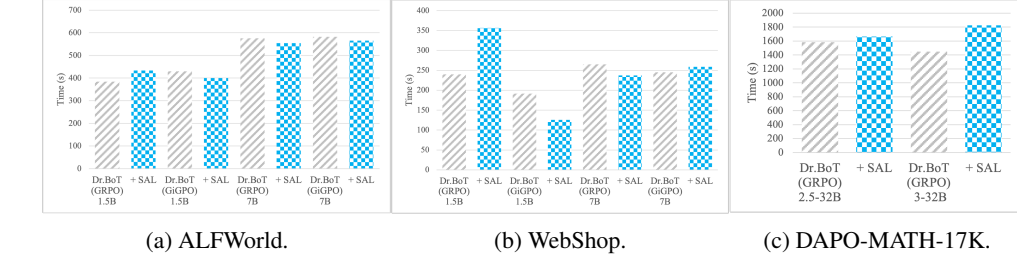


Figure 14: The averaged policy training time (s) per step with and without the proposed SPEAR.

We compare the computational complexity of our SPEAR with the vanilla GRPO algorithm in Table 10. Most of the computation comes from the forward and back-propagation of the filtered samples in the replay buffer. The memory operations such as the update and filtering of the buffer are light-weight and can be simply ignored. Given the current experimental settings (see Table 8), we observe that $n_{\text{SIL}} \approx 0.5$ for ALFWorld and WebShop, and $n_{\text{SIL}} \approx 0.33$ for DAPO-MATH-17K. In this case, our SPEAR additionally introduces around 10% ~ 25% computation overhead with $K \leq G$. Such computation complexity is acceptable in practice as the time of each training iteration is dominated by that of on-policy rollout generation.

Figure 14 shows the runtime per iteration step with and without the proposed SPEAR across different tasks and model scales. the total optimization procedure (including the rollout generation, advantage computation, log-probability inference, reward computation, and the actor update) is quite similar on average for ALFWorld, WebShop, and their SPEAR counterparts. For ALFWorld and WebShop, the 1.5B models exhibit larger variance than 7B models in training time. We believe such variance is associated with findings of the previous study (Havrilla et al., 2024) that the size of LLMs matters to the exploration diversity. Smaller LLMs are less diverse in exploring strategies due to their shallower reasoning nature, and are therefore prone to suboptimal policies with relatively increased stochasticity in training dynamics. For DAPO-MATH-17K, an increase around 5% and 26% is observed respectively on Qwen2.5 and Qwen3 models. Since the time per step is dominated by the rollout generation and actor update, we believe such increase in time is caused by the longer reasoning traces, more tool call interactions, and the additional iterations from the replay buffer. Such encouraged exploration by SPEAR is exaggerated on the reasoning model Qwen3 and leads to longer training time.

2052 It is noted that the proposed SPEAR does not increase GPU memory usage. The introduction of
 2053 the experience replay buffer is equivalent to increasing the training batch size per step. Due to the
 2054 current sequential implementation that uses gradient accumulation with a fixed mini training batch
 2055 size, we can achieve policy optimization on batches of any size without OOM issues.
 2056

2057 **A.16 FUTURE WORK**

2058 **A.16.1 DYNAMIC SCHEDULING**

2060 In the future, one of the promising research direction is to model and adjust the scheduling param-
 2061 eters dynamically. It is noted that there exists no clear-cut line between exploitation and explo-
 2062 ration during training (Snoek et al., 2012; Wang et al., 2018). The exploitation and exploration are
 2063 intertwined and optimized together, which is often context-dependent (Bellemare et al., 2016) or
 2064 guided by the policy itself (Pathak et al., 2017). Therefore, the scheduling should be progressive
 2065 and smooth. We believe three kinds of techniques can be utilized for guiding the exploration:
 2066

2067 **Entropy as the medium.** Following ARPO (Dong et al., 2025b), we could schedule the self-
 2068 imitation and intrinsic reward with monitoring of the entropy itself. It is direct and intuitive, and
 2069 it allows flexible and frequent adjustments. However, the modeling of the relationship between
 2070 policy entropy and scheduling itself is often task-dependent and parameter-involved, introducing
 2071 additional computation. In addition, the entropy is prone to noise where outliers of certain tokens
 2072 might interfere with the scheduling negatively.

2073 **Performance as the medium.** One could also adjust the scheduling by the performance-related
 2074 metrics (Agrawal & Goyal, 2012) such as the task completion rate and the number of tool-calls.
 2075 The association between exploration and success rate can be utilized. Furthermore, the number of
 2076 tool-calls often indicates the degree of exploration with the environment. Nevertheless, the metrics
 2077 might be deceptive as an early stop of exploration stimulation could lead to suboptimal convergence.
 2078

2079 **Curiosity or Self-confidence as the medium.** One could intensify the exploration when the policy
 2080 exhibits uncertainty (Pathak et al., 2017; Ladosz et al., 2022) about its actions or confusion about the
 2081 transition of environment states. The policy’s familiarity of the environment and its action reflects
 2082 the exploration status. But it often requires parameterized learning of the curiosity or confidence via
 2083 quantification of the inconsistency between the expected state transition and the real one.

2084 **A.16.2 STEPWISE CREDIT ASSIGNMENT**

2085 In a extremely noisy tool ecosystem, the discrimination between good and bad experience is rather
 2086 challenging merely with the outcome reward (Deng et al., 2025; Zeng et al., 2025). Under such
 2087 circumstance, a process reward model (PRM) would be beneficial to provide fine-grained, stepwise
 2088 supervision. However, it remains prohibitive to conduct manual evaluation and preference annota-
 2089 tion for training online PRMs. Very recent studies highlight a few potential directions:
 2090

2091 **The usage of meta-reward via LLM-as-a-Judge.** Instead of training a process reward from
 2092 scratch, one could directly use an off-the-shelf LLM to assess each step not from the accuracy
 2093 but from the aspect of meta-reasoning (Zhang et al., 2025b) behaviors (e.g., planning, exploration,
 2094 and reflection).

2095 **The employment of implicit PRMs.** One could derive an implicit PRM (Cui et al., 2025a) by
 2096 reparameterization of the outcome reward as a sum of log-likelihood ratios of two LLMs over steps.
 2097 Therefore, the step-wise reward can be approximated as the differences between two adjacent steps
 2098 (agent actions) (Liu et al., 2025a)

2101 **The introduction of world models.** The noise from real-world tool ecosystem might be inevitable
 2102 and therefore it is reasonable to perform a model-based sim2real RL (Moerland et al., 2023). One
 2103 could prepare an internal world model to deliver reliable state transition (Gu et al., 2024) for tool-
 2104 based interaction, which help the agentic LLMs develop strategies via RL. Then, the trained LLM
 2105 further adapts to real environment after a few more steps of training to gain robustness against noise.

2106 A.17 THE USE OF LARGE LANGUAGE MODELS
21072108 In the present study, we use the LLMs for the polishing of the manuscript writing and the discussions
2109 for analysis.
2110
2111
2112
2113
2114
2115
2116
2117
2118
2119
2120
2121
2122
2123
2124
2125
2126
2127
2128
2129
2130
2131
2132
2133
2134
2135
2136
2137
2138
2139
2140
2141
2142
2143
2144
2145
2146
2147
2148
2149
2150
2151
2152
2153
2154
2155
2156
2157
2158
2159